1998

Controlling toolholder fretting through design modification.

Joseph. Jouraij
University of Windsor

INFORMATION TO USERS

This manuscript has been reproduced from the microfilm master. UMI films the text directly from the original or copy submitted. Thus, some thesis and dissertation copies are in typewriter face, while others may be from any type of computer printer.

The quality of this reproduction is dependent upon the quality of the copy submitted. Broken or indistinct print, colored or poor quality illustrations and photographs, print bleedthrough, substandard margins, and improper alignment can adversely affect reproduction.

In the unlikely event that the author did not send UMI a complete manuscript and there are missing pages, these will be noted. Also, if unauthorized copyright material had to be removed, a note will indicate the deletion.

Oversize materials (e.g., maps, drawings, charts) are reproduced by sectioning the original, beginning at the upper left-hand corner and continuing from left to right in equal sections with small overlaps.

Photographs included in the original manuscript have been reproduced xerographically in this copy. Higher quality 6" x 9" black and white photographic prints are available for any photographs or illustrations appearing in this copy for an additional charge. Contact UMI directly to order.

Bell & Howell Information and Learning
300 North Zeeb Road, Ann Arbor, MI 48106-1346 USA
800-521-0600

UMI®

Controlling Toolholder Fretting Through Design Modification

by

Joseph Jouraij

A Thesis

Submitted to the Faculty of Graduate Studies and Research

through the Department of Mechanical Engineering

in Partial Fulfilment of the Requirements for

the Degree of Master of Applied Science at the

University of Windsor

Windsor, Ontario, Canada

1998

Abstract

During machining, cutting forces exerted on a toolholder will cause its shank to bend within the spindle. If the shank's deflections are larger than the gap separating the two surfaces, impacting will occur. The repetitive impacting motion between the spindle and toolholder results in a fretting condition. Over time, this will lead to wear and corrosion damage that is costly to repair and can potentially affect machining performance.

Typical means of dealing with fretting include the use of surface treatments such as coatings or the use of wear resistant materials. However, these are only treatments and not solutions. Although they may reduce fretting damage, they do not prevent the fretting condition. The proper solution would be to prevent the contact that causes the fretting.

Through finite element simulations and experimental testing, modal analysis was performed on various toolholder designs. Since different designs will have different dynamic characteristics, the goal was to find those designs that would minimize shank deflections, and thus minimize fretting damage.

Two types of toolholders were studied: straight shank and tapered shank. The design of each was altered by varying the overall length and diameter. Within typical operating frequencies, it was generally found that shank deflections were less in tapered designs than in straight designs and that the deflections decreased as the length of the toolholder decreased. Increasing the diameter had no significant effect on deflections. By understanding how design modifications can affect shank deflections, a toolholder can be created to minimize the chance of fretting.

Dedication

To my parents, sisters and brothers.

Acknowledgments

I wish to express my sincere appreciation to Dr. R. Du, whose advice and guidance helped me throughout this project. I would also like to thank him for providing the resources that made the completion of this work possible. Special thanks to Dr. W. North and Dr. J. Yang for their advice and comments, as well as to N. S. Chana for all his time and never ending patience in answering my technical questions. Finally, I would like to thank Ford Powertrain Operations for their funding of this work.

Table of Contents

List of Figures

List of Tables

I. Introduction

When the shank of toolholder is inserted into a spindle, a very small clearance remains between the adjoining surfaces. During operation, vibrations and cutting loads will cause the shank to bend. If the resulting deflections are greater than the clearance, impacting will occur between the two surfaces. Repetitive impacting over a small displacement amplitude is referred to as a fretting condition. Over time, this can lead to wear and corrosion damage on both surfaces. This is generally not a concern with toolholders, since they are relatively inexpensive and easily replaced. However, a spindle is a high cost, precision component that is an integral part of a machine tool operation. Corrosion and wear damage will not only affect the spindle's performance, but may shorten its life span. Therefore, it would be desirable to eliminate the fretting problem.

A. Objective

Since the fretting condition is caused by vibration, it is proposed that fretting can be controlled by altering the dynamic characteristics of the toolholder. Realizing that fretting is a result of shank deflections and that the dynamic characteristics of the toolholder depend on its design, the objective of this thesis, restated more specifically, will be to show that shank deflections can be controlled by altering the toolholder's design.

B. Thesis Organization

This thesis has been organized in such a way as to introduce the necessary background information before dealing with the issue at hand. Chapter II contains general information about toolholders and fretting, as well as reviews of work done in the

area of fretting. Chapter III deals specifically with fretting in toolholders and spindles. Causes and potential problems are discussed and possible solutions are reviewed. Chapter IV contains the analysis work that was conducted using computer simulations and experimental testing, while Chapter V details how actual physical responses were calculated. Finally, conclusions are given in Chapter VI.

II. Background

Before discussing the problem of toolholder fretting, some background information is provided to give the reader a general understanding of toolholders and fretting. A literature review is supplied to provide additional insight into the fretting phenomenon.

A. Toolholders

A toolholder is a device that holds the cutting tool. Many different types of toolholders are in use today including straight and tapered shank designs, as well as HSK and ABS designs. Despite the diversity, all toolholders have these common elements: a retention stud or threaded hole on one end, an external 'alignment' taper that nests in an internal spindle taper, a keyway that drives the toolholder and a means for holding a tool shank. See Figure 1 for an illustration.

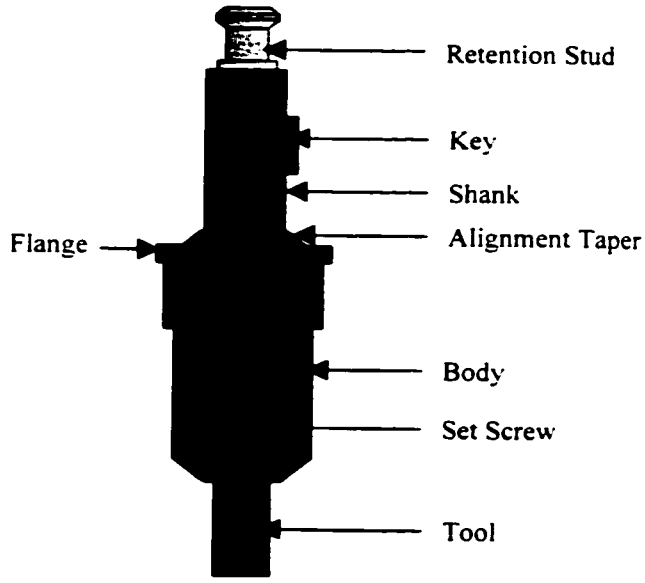

Figure 1 - Common Elements on a Toolholder

When the toolholder is inserted into the spindle, a mechanism of some sort clamps onto the retention stud and pulls the alignment taper firmly against the spindle taper. The other end of the toolholder usually has a socket for a collet that grips the cutting tool shank. Collets come in a variety of internal diameters so many tool shank sizes can be used by the same toolholder. A simpler, but less versatile, configuration is a single hole in the toolholder with a setscrew to hold the tool shank. Some manufacturers make the cutting tool and toolholder a single element for applications where precision is high and the cost of scrapping the entire holder when the tool fails, is acceptable.

An important consideration with respect to toolholders is correct balancing. Toolholders that are balanced will be able to provide the performance and accuracy needed in most machining operations. In addition to improving performance, balanced toolholders also minimize wear on the spindle bearings. Balancing a toolholder is only one step in assuring proper conditions for precision machining. It is equally important to consider the balance of the tool, how the tool in mounted in the toolholder, how the toolholder is mounted in the spindle and the conditions of the spindle and spindle bearings. Potential causes of imbalance include:

1) Worn spindle or spindle bearings – Vibration can be created by worn spindle bearings which will cause the toolholder/spindle to wobble as it rotates (see Figure 2). This vibration will prevent the cutting tool from making a smooth cut and makes it difficult to hold close tolerances.

2) Eccentricity – Can be caused by either components that are not mounted on center or by components that are bent or warped. The cutting tool must be concentric with the toolholder and the toolholder must be concentric with the

spindle. How much they are off-center (represented as 'e' in Figure 3) is a major factor contributing to imbalance.

3) Toolholder taper – Toolholders have an alignment taper which is designed to locate them precisely within the spindle. However, "standard" tapers are not always machined as accurately as expected. "Slop" in the taper fit will allow the toolholder to shift positions during machining as shown in Figure 4. This shifting will prevent the toolholder assembly from remaining in balance. It is important that the taper on the toolholder match the taper of the spindle exactly.

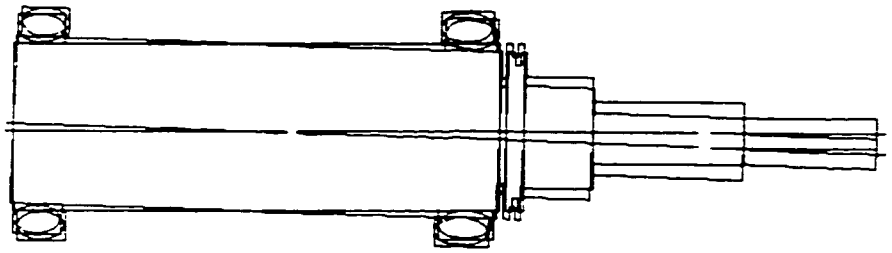

Figure 2 – Vibrations Resulting from Worn Spindle Bearings

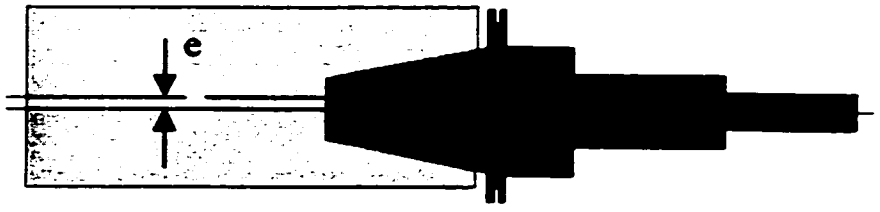

Figure 3 – Eccentric Toolholder Mounting

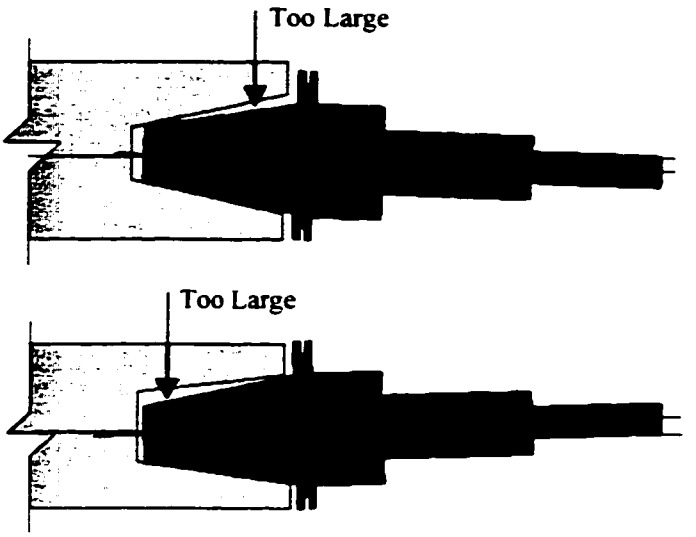

Figure 4 - Improper Toolholder Fit Results in 'Slop'

B. Fretting

A fretting condition refers to any situation in which the contacts between materials are subjected to a low amplitude oscillatory sliding/impacting motion. Fretting often occurs when surfaces, which are intended to be fixed in relation to one another, still experience a small oscillatory relative motion. Fretting often takes place in hubs and disks press fitted to rotating shafts, in riveted and bolted joints, between strands in wire ropes and between the rolling elements and their tracks in bearings.

There are several different classifications of fretting damage. These include fretting fatigue, fretting corrosion and fretting wear. There are also many variables which control fretting conditions. These include normal and tangential loads, slip (or displacement) amplitudes, frequency, temperature and humidity.

Fretting maps have been developed that relate the key variables (load, displacement, frequency) to the different types of fretting damage as shown in Figure 5. Region I

represents the low damage area. In this area, there is very limited surface damage by oxidation and wear. In region II (fretting fatigue), wear and oxidation effects are small, but crack nucleation and growth significantly reduce fatigue life. In region III, crack formation is limited, but severe surface damage is caused by wear (fretting wear) and assisted by oxidation (fretting corrosion).

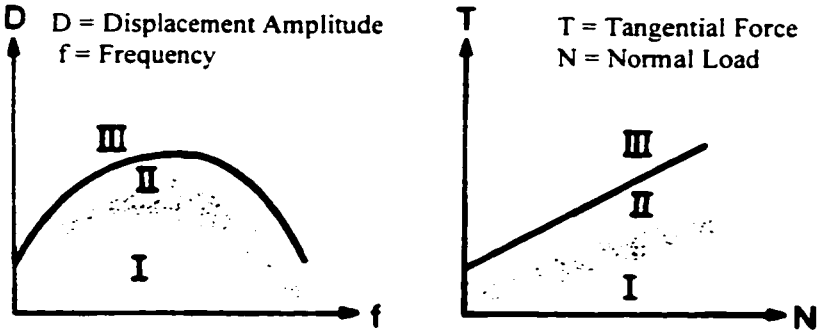

Figure 5 – Fretting Maps [22]

C. Literature Review

There is no known work dealing specifically with fretting in toolholders, but a great deal of research has been done in the area of fretting. Research that could provide some insight into toolholder fretting is discussed here.

1. Tube Fretting In Heat Exchangers

Research that relates very closely to toolholder fretting was done by P. L. Ko [14] who studied fretting wear in heat exchanger tubes. The tubes where flexing due to flow induced vibration and, as a result, were impacting and/or rubbing against their supports. The obvious solution would be to reduce the flow rate, but high flow rates are desirable for improving heat transfer and reducing the fouling rate.

Ko discovered that due to the clearance between the tube and the tube support, the vibrating tube can repeatedly make and break contact with the support. Depending on flow conditions, a tube may be rubbing and impacting against the tube support or, alternatively, it may be simply rubbing with very little or no separation. The latter is the result of a high static normal force and low amplitude vibration. This can occur if the tube is firmly pressed against one side of the tube support due to tube/support eccentricity and/or tube bow. Rubbing can also occur from the bending and thermal expansion of the tube. This will cause axial rubbing as well as rocking between the tube and support. However, as Ko points out, it is the combination of rubbing and impacting that usually causes the worst damage. Figure 6 illustrates severe fretting damage on a tube.

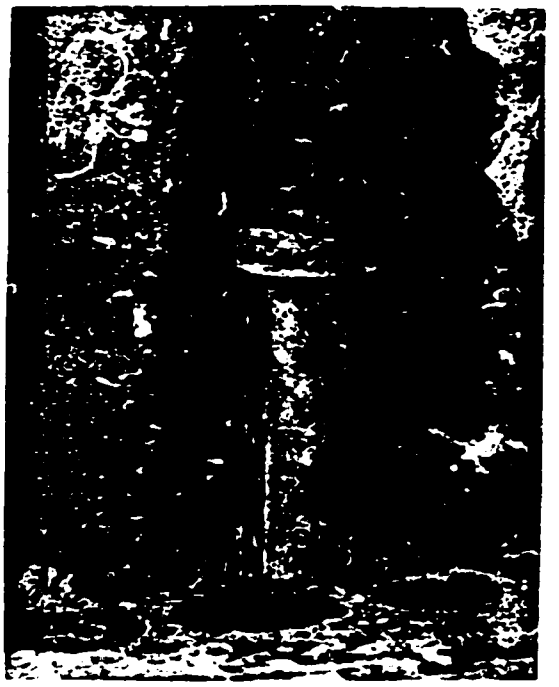

Figure 6 – Fretting Damage in Heat Exchanger Tube [14]

The sensitivity of wear rate to various system parameters were studied and include the following:

1) Tube/Support Clearance – It was found that wear rate is very sensitive to the clearance. With a constant excitation, the wear rate increased as the clearance increased. The wear rate dropped off when the tube-to-support contact could no longer be maintained by the excitation. The conclusion drawn was that fretting damage can be reduced by making the clearance as small as possible.

2) Tube Support Area – The thickness of support plates can vary. Tests showed that the wear rate increased with reduced tube support area. It was concluded that maximizing the tube support area will reduce fretting damage.

3) Material Combination and Hardness – It was found that similar materials should not be used for both contacting surfaces as very high wear rates can occur. It was also discovered that the hardness of the material, by itself, does not have a significant effect on tube wear. Studies have shown that various steels of the same hardness had wear rates that varied by more than ten fold. Therefore, care should be taken to ensure compatibility between the tube/support materials.

Other parameters that were shown to affect wear rate include type of tube motion (impacting or rubbing), frequency of vibration and support impact force.

Using a finite element analysis program, Ko's analysis of the problem included solving for natural frequencies and mode shapes of the tubes. When simulated fluid-induced forces were applied, the displacement of the tubes could be calculated. Then, by combining the results of the software with experimental wear data, the wear rate, and thus the life of the tubes, could be estimated.

2. Polymer Coating Life

One method typically used to prevent fretting damage is to apply a polymer coating to the metal surfaces. This will later be reviewed as a possible treatment for toolholder fretting. For a coating to be effective it must (a) not wear through and let metallic contact occur and (b) not cause damage to the metals on which they are sliding. Research was conducted to investigate the effect of applied load and relative humidity on the durability of polymer coatings. This research was conducted by P. A. Gaydos et al. [8]. The fretting wear of the coatings was studied as a function of polymer composition, operating conditions (load, amplitude, frequency), environment (air, relative humidity) and coating thickness. The tests were conducted by fretting a steel ball against a polymer coated steel surface. In general, for all polymers, the coating life decreased with increased load. However, the magnitude of the decrease varied considerably. At low humidity, some polymer coatings experienced a decrease in life by a factor of 1000 while others dropped by only a factor of three. At higher humidity, the coating life varied depending on the polymer.

It should also be pointed out that with some of the coatings that contained chlorine, the steel ball experienced a significant loss of material at the contact area. The mechanical stresses and the presence of iron in the fretting interface caused the polymers to degrade by a process of dehydrochlorination. The hydrochloric acid generated in this process not only promoted additional degradation, but it also attacked the steel.

3. Effects of Oxide Debris on Fretting

During fretting wear, material loss from the contacting surfaces will become oxidized (fretting corrosion) resulting in the production of considerable amounts of very

fine iron oxide debris. This debris has been studied by A. Iwabuchi [12] to evaluate its role in the fretting wear of steel. Iwabuchi states that in considering the wear mechanism of fretting, the role of oxide particles is important. It is claimed that the removal rate of oxide from the interface governs the wear rate, rather than the formation rate of oxide. Consequently, a significant factor governing fretting wear is the behaviour of the oxide particles.

In experiments conducted, oxide particles (αFe_2O_3) were artificially supplied between the surfaces before fretting. The tests showed two different situations resulting from the use of the particles. The first was the abrasive action which accelerated the wear rate. This is due to the higher hardness of oxide debris than that of the bulk material. The second was the protective action which reduced the wear damage. This was due to the formation of a compacted oxide layer at the interface. Such a layer was called the "third body" and it had the load carrying capacity to prevent metal-to-metal contact. Which situation appeared depended on fretting conditions such as normal load and slip amplitude. Generally, the removal rate of the oxide from the interface increases with the increase in the normal load and the slip amplitude. From the point of view of reducing fretting damage, how wear debris can be maintained between the surfaces is important. If the oxide particles remained compacted, the particles showed the protective action. On the other hand, if the wear debris moved around at the interface as loose particles (as it usually does in the early stages of fretting), the particles caused the abrasive action.

III. Toolholder Fretting

The following sections will deal specifically with toolholder fretting. The first section will describe the mechanism of toolholder fretting. Later sections will discuss the problems that result from fretting damage, as well as some possible solutions or treatments.

A. Cause

When a toolholder is inserted into a spindle, a clamping mechanism of some sort pulls the toolholder tightly inside the spindle pocket. This is to ensure that the external taper of the toolholder nests firmly against the internal taper of the spindle. However, there is a small gap that is left between the shank and the spindle wall. Figure 7 illustrates this with a tapered shank toolholder. It is interesting to note that, although the taper is standardized, the diameter of the shank is left up to the individual manufacturers. Thus, the size of the gap could vary slightly depending on the toolholder [16]. The gap size is usually in the range of 0.02 mm to 0.04 mm.

During machining, cutting forces on the tool induce vibrations in the toolholder. This, in turn, causes the shank to deflect. Figure 8 illustrates how the toolholder will flex under a load. During cutting, the magnitude and direction of the forces will vary as each tooth on the tool cuts through the metal. It is this variability in the forces that will cause the deflections to oscillate about some mean value. If the deflection of the shank is larger than the gap spacing, impacting will occur. The constant impacting (and some rubbing if the toolholder twists) between the spindle and shank results in a fretting condition.

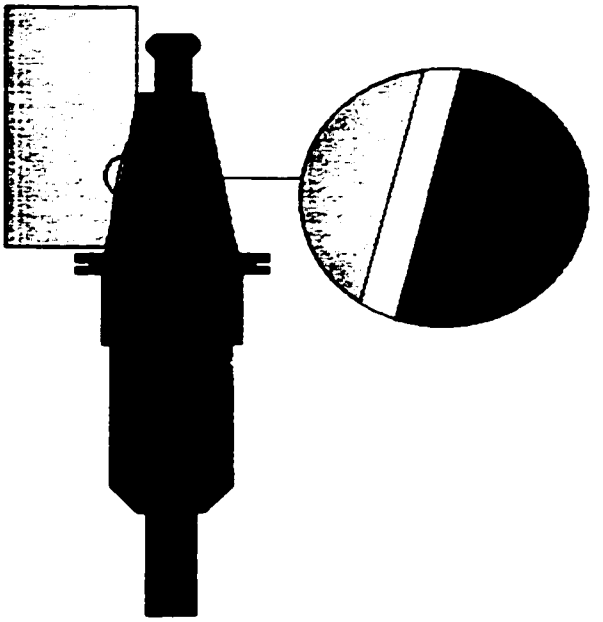

Figure 7 – Clearance Between Shank and Spindle

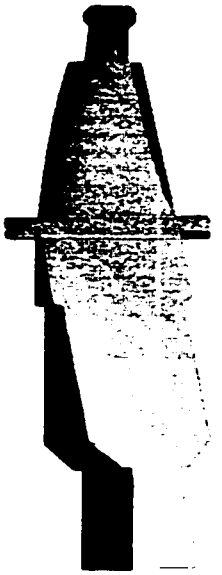

Figure 8 – Flexing of Toolholder under Load

Two different (yet related) fretting types can occur as a result of this fretting condition: fretting wear and fretting corrosion. Fretting wear will occur when metallic contact causes the adhesion between asperities on the two surfaces and forms metallic

wear particles. These particles will then be fragmented and oxidized in the presence of oxygen (fretting corrosion). The wear rate subsequently increases as a result of the abrasion caused by the oxide particles. For steel vibrating against steel in air, the main symptoms of fretting corrosion are the production of voluminous amounts of loose αFe_2O_3 (ferritic iron oxide) and the presence of brown films on the surfaces after the debris is removed. Other metals and environments give different debris. The identification of αFe_2O_3 by X-Ray diffraction is proof of fretting corrosion of steel [9].

Figures 9 and 10 show fretting damage on the straight shank toolholders. In Figure 9, most of the damage is confined to the upper portion of the shank with a little damage near the bottom. The damage resembles rust stains with the characteristic brown colour. This is a sign of fretting corrosion. Closer examination of the damage reveals shiny spots that surround the rust damage. The shiny appearance on the surface is indicative of impacting. This was perhaps the first stage of the damage with corrosion occurring later. Figure 10 is an identical shank with far worse surface damage. Examination of the shank reveals that some areas are much darker in discolouration than others, indicating a further progression of corrosion.

There are some common features to both shanks. There is no damage where the key slot runs from the base of the shank to the top. This is, of course, because there is no contact in this area. Also, note the damage on the alignment taper of each shank. The taper is firmly pressed against the spindle's taper and there is no chance of impacting damage, however, some looseness between the key and key slot may allow the toolholder to twist slightly in the spindle. The fretting damage results from the rubbing between the two surfaces.

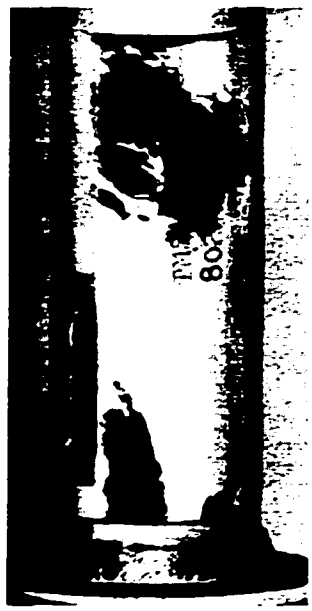

Figure 9 – Mild Fretting Corrosion

Figure 10 – Severe Fretting Corrosion

For comparison, Figure 11 illustrates fretting corrosion on a bearing ring. In high load applications, the ring can move in its mounting during bearing rotation. Note the similarities of the damage to the toolholders. There are dark corrosion products at A, surrounded by polished areas at B. There is also a round unfretted spot at C where a hole in the housing prevented contact [19]. Figure 12 is yet another example of fretting corrosion in a grease testing apparatus. In this case, a bronze ring was loaded and oscillated against the shackle in the presence of a grease [9]. The damage is strikingly similar to that of the toolholders.

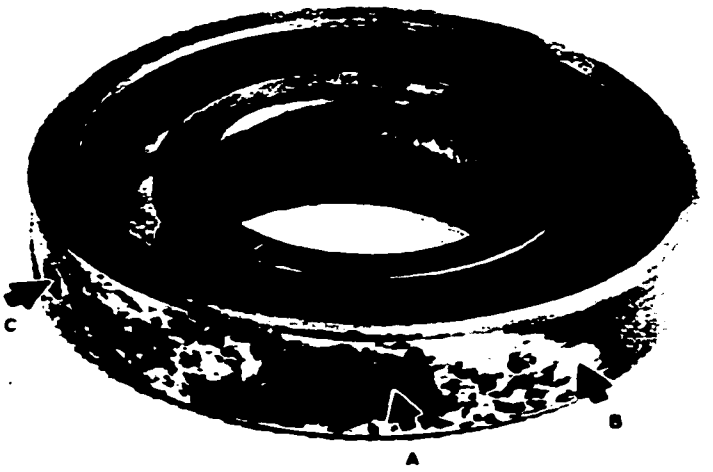

Figure 11 – Fretting Corrosion of Bearing Ring [19]

Figure 12 – Fretting Corrosion of Grease Testing Shackle [9]

B. Problem

Fretting wear and corrosion results in surface degradation and limits the life of the components. Over time, the wear and corrosion on the spindle's surface will alter its dimensions. The clearance between the toolholder shank and spindle will increase

resulting in "slop", which was previously explained. For precision machining, the toolholder must remain perfectly aligned within the spindle. With an increase in the gap spacing, there is a chance the toolholder could shift positions. This is a particular concern with longer toolholders. If the shank were to tilt slightly from the spindle's centerline, that small deflection will result in a greater deflection at the tool tip as shown in Figure 13. A toolholder that is not concentric with the spindle will wobble, considerably affecting the surface finish of the machined part.

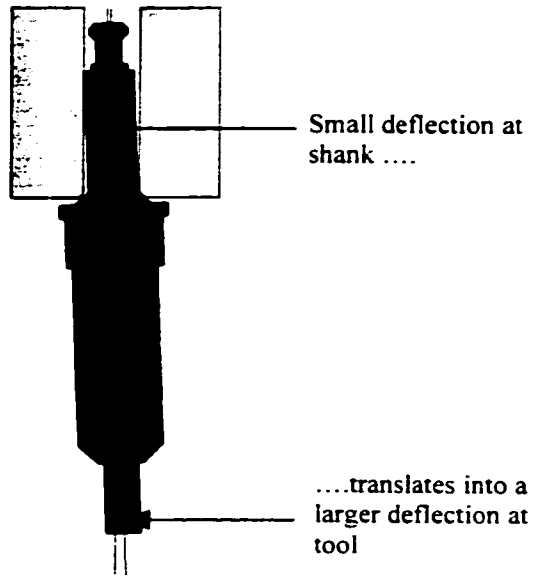

Figure 13 – Tool Tip Deflection as a Result of Slop

In addition to reduced surface quality, maintenance and performance issues arise. A wobbling toolholder generates an out-of-balance force that increases with the square of the spindle speed. This force can become quite considerable and will put a great deal of unnecessary stress on the spindle's bearings. The result is that the bearings will prematurely wear, decreasing spindle performance and increasing downtime for maintenance.

C. Possible Solutions

This section will discuss some possible solutions to fretting damage. Along with the research discussed in the literature review, the viability of these solutions with respect to toolholder fretting will be assessed.

1. Eliminate Gap Spacing

Referring back to the problem of tube fretting in heat exchangers, it was stated that fretting damage worsened as gap spacing increased. Thus, the gap should be as small as possible to reduce/prevent any relative motion between the surfaces. This would require the use of a press fit, where the two surfaces are held together with a high normal force. In fact, the reduction of fretting damage in bearings is often achieved by increasing the press fit between the moving parts. This would serve to reduce the relative motion between them. However, such a situation would not be feasible for toolholders. For a press fit to work, the shank would have to be slightly larger than the spindle pocket. This would make manual or even automatic assembly impossible without first chilling or heating one of the components.

2. Use of a 'Third' Body

In Iwabuchi's studies, it was shown that oxide debris had the ability to hinder further wear once it was compacted. Toolholders are usually not left within the spindle for great lengths of time, so the chance of enough oxide debris accumulating is slim. However, this raises the question of using another material to prevent metal to metal contact. Some possibilities might include an oil film or even a thin rubber gasket. Unfortunately, due to the large loads that would be exerted by the toolholder, and the

nearly zero clearance, the material would probably wear through and disintegrate rather quickly. In the case of oil, an extreme pressure oil would be needed and the toolholder/assembly would need to be redesigned to contain the liquid. As a result, the use of a buffer material does not seem feasible.

3. Surface Treatments

The use of polymer coatings on metal surfaces is a popular technique of reducing fretting damage. It acts like the 'third' body by preventing metal to metal contact, but it is applied directly to the metal surface. However, as pointed out in the literature review, these coatings work only in low load applications and wear out rather quickly as contact load increases. Also, environmental conditions such as excessive relative humidity limit the life of a polymer coating.

A more suitable technique would be the use of a hard-surfacing material. Hard-surfacing is a process by which an alloy coating is welded, fused or sprayed onto the surface of a metal part. It is used to provide a variety of desired properties including wear resistance, corrosion resistance and strength. For fretting conditions, the use of a cobalt-based hard-facing alloy is recommended as it is extremely resistant to galling [5]. A drawback to this process is the added expense of the coating.

IV. Finite Element Analysis

The use of a surface treatment is a typical method of working around the problem of fretting, however, it is not a solution. Although its use may reduce or possibly prevent fretting damage, it does not prevent the fretting condition. The proper solution is dictated by the correct diagnosis of the problem. For example, if wear was caused by abrasion, the solution would be to remove the abrasive. Toolholder fretting is a result of the shank and spindle impacting; preventing the contact would be the solution. Since this is clearly a vibration related problem, the objective of this work is to determine how the dynamics of the toolholder affect the deflection of the shank. By limiting the deflection, it is hoped that fretting can be controlled.

SDRC's I-DEAS finite element analysis software was the primary tool used in evaluating the toolholder's dynamics. A toolholder can be modeled, meshed and solved (for normal mode dynamics) in a relatively short period of time. Using the I-DEAS Model Response package, forces simulating cutting could be applied and the resulting deflections of the shank found. If the deflections are too great, the toolholder could be redesigned and the new deflections found.

A. Creating the Model

The basis of any FEA work is the creation of a good model. This includes defining the proper mesh type and density, the proper boundary conditions and the proper geometry (although the model does not have to look anything like the actual component to produce good results). A model is usually considered to be good if it can produce results that are reasonably accurate (at least in the range of interest). It is hard to quantify

what 'reasonably' means because some systems can be more accurately modeled than others. For instance, there are certain physical conditions that simply cannot be modeled and either must be left out or modeled in some other way. An example is the inability to model gaps or any looseness between assembled components under dynamic conditions. Under these circumstances there is usually no choice but to accept the errors introduced from simplifications. Sometimes simplifications and assumptions are needed to avoid creating a model that is too complicated (with a very large number of elements). This may result in the loss of some accuracy, but the time saved in reduced computations makes it acceptable. It is ultimately up to the engineer to decide what is reasonable and acceptable.

The creation of the toolholder models (straight and tapered shanks) begins by making a necessary assumption. The toolholder is actually an assembly of various components including a retention stud, set screw (or collet) and the tool itself. Since any looseness between the components cannot be modeled, it will be assumed that all the parts are assembled together very tightly (and remain that way during operation) so that the toolholder behaves as a single body. Also, since a dynamic analysis is being performed, it will not make a difference to the end result if small details are left out. These may include such things as the tool's teeth, beveled edges, exposed threads, small grooves and any other small feature that does not affect the overall structure. Leaving these features out will greatly simply meshing in those areas and will reduce the number of elements needed. The benefit is reduced computational times with a negligible loss of accuracy.

Designing a model in I-DEAS is a relatively simple task. The toolholder designs basically consist of cylinders and cones of various sizes that are assembled together to form the basic shape. Figure 14 illustrates the two toolholder designs that will be analyzed. Since many different sizes of each toolholder will be created to study the changes to its dynamic behaviour, many of the model's dimensions were constrained to one another. For example, the outside diameter of the toolholder's body is related to the inside diameter, as well as to the flange diameter in the tapered design. If a larger outside diameter was required, the other dimensions would change automatically to compensate for the difference. Relating dimensions in this way and specifying a few key dimensions, on which all others are based (often called parametric design), makes modifications a simpler task. Once the model is complete, altering the toolholder's overall length and

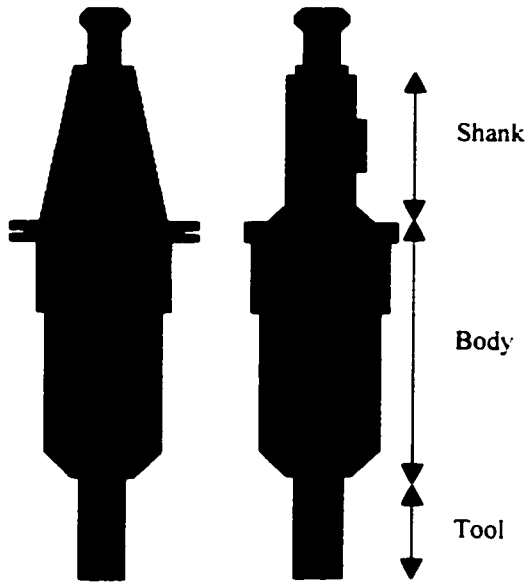

Figure 14 – Tapered and Straight Shank Toolholder Designs

diameter would only require making changes to the key dimensions.

The next step of the process is to apply a mesh to the model. There are many different types of meshes that are available for use. Shell elements are applied to the surface of a part and have a defined thickness. These elements are typically used for thin walled parts such as tubing, and would not be appropriate here.

Another type of mesh is the beam element. Unlike some other mesh types, the beam element does not require any pre-drawn model on which to apply the mesh. Rather, beam elements of various cross-sectional shapes (circular, rectangular, oval) and sizes are linked together to form the part. Each element has two nodes which connect it to other elements. Figure 15 illustrates how a toolholder can be represented by these elements. The great advantage of beam elements is quick computation times due to the small number of nodes. However, there are drawbacks. All the nodes are located along the centerline of the toolholder, making it impossible to apply constraints or forces to the outside surfaces of the part. Also, features such as a key cannot be added to the surface. As a result, beam elements also would not be appropriate for this analysis.

The final choice is the use of a solid mesh. Solid meshes can be applied to just about any type of geometry on a solid part. Difficulty arises when trying to mesh parts with very sharp corners or too great a curvature since the elements can become quite distorted. The main disadvantage with solid meshing is the great deal of nodes that are usually required to properly represent a part, resulting in long computation times. Nevertheless, its ease of use makes it very popular. Common solid mesh elements include brick, tetrahedral and pyramid. Each of these can also be broken down into linear or quadratic. As seen in figure 16, a linear tetrahedral element has 4 nodes, while a quadratic has 10 nodes. More nodes along the length of an element allow for greater

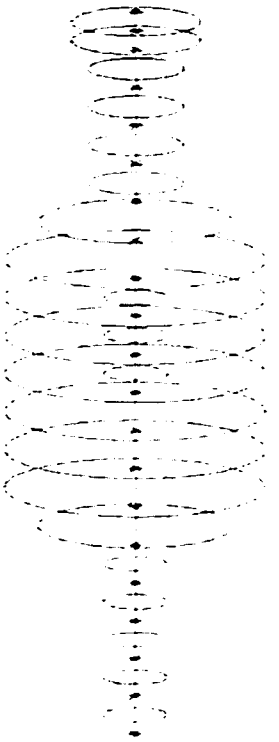

Figure 15 – Model of Toolholder using Beam Elements

accuracy but increase solver times. Since quadratic tetrahedral elements yield better results, they will used for the analyses.

I-DEAS has two options on how to mesh the part; mapped (manually done) or free (automatically done). Mapped meshing is best suited for parts with simple geometry, while free meshing is used on more complex parts. The latter is usually recommended because it allows the FEA package to optimize the mesh. It is this option that will be used to mesh the various toolholder designs.

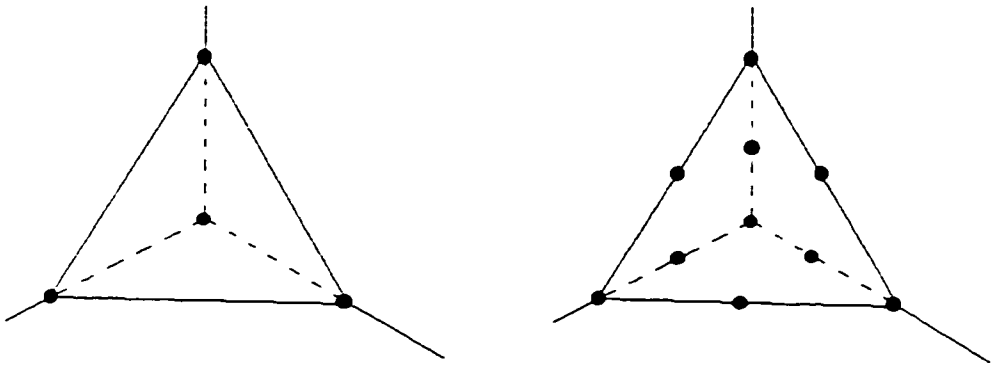

Figure 16 – Linear and Quadratic Tetrahedral Elements

The last parameter needed before beginning the meshing procedure is the mesh size (or element size). This is an important variable because an inadequate mesh density in all or certain parts of the model will not provide good results. A compromise needs to be found, however, to balance between required accuracy and computation time. A mesh density that requires ten hours of computation, but yields a difference of only a few percent over one that requires two hours is probably not a better choice. At the other end of the spectrum, an element size too large may result in a model that produces erroneous results. An optimum size can be found by running many simulations with decreasing element sizes until the result converges. Increasing the mesh density after that would be pointless. Table 1 summarizes several element sizes that were tested and the results that were obtained under free vibration conditions. It is clearly seen that the difference in results is negligible and that the 10 mm element size would be quite adequate for the simulations. However, that size tended to result in many distorted elements and required more work to correct (re-meshing was sometimes necessary). Therefore, the 8 mm element size will be used for all the toolholder simulations.

Element Size (mm)	Mode 1 (Hz)	Mode 2 (Hz)	Mode 3 (Hz)
6	4112	5151	7685
8	4122	5165	7696
10	4131	5171	7709
Max. Difference (%)	< 1	< 1	< 1

Table 1 - Effect of Element Size on Simulation Results

B. Verification of the Model

Typically, once a model has been meshed, the next step would be the application of the boundary conditions. However, it would be a good idea to verify whether the mesh density and type were indeed adequate by comparing the FEA results with actual (experimentally found) results. Small differences might show that the mesh needed slight adjustment in some areas while significant differences might indicate that the mesh needed complete reworking.

The experimental work is conducted using impact testing, a widely used method of excitation for structural frequency response testing, otherwise known as modal analysis. Its popularity is mainly due to the simplicity of the method which makes it adaptable to a wide range of testing conditions. The basic procedure uses an impact hammer to apply a force to the structure through a load cell. The response is then measured by a suitable response transducer (accelerometer). After passing the force and response signals through signal conditioning equipment (amplifiers, filters), the signals are digitized and then Fourier transformed. The final result is a plot of the frequency response function (FRF) which is a ratio of the system's response to the force input. An FRF measurement made on any structure will show its response to be a series of peaks. These peaks are often sharp, with identifiable center frequencies indicating that they are resonances

(modes). The identification and analysis of all the resonances in a structure's response is the basis of modal analysis.

One important assumption that must be made is linearity. Only systems that behave linearly (response is proportional to input) can be tested. This has some implications for frequency response functions. The first is that the measured FRF is independent of the excitation level and the second is that the measured FRF between any two points on the structure is independent of which of them is used for response or excitation.

The verification process will compare FEA results under free vibration with those found experimentally. The 'free' condition meaning that the test object is not fixed to ground at any point and is, in effect, floating in space. In this condition, the structure will theoretically exhibit 6 rigid body modes (no bending or flexing at all) and each of these modes will have a natural frequency of 0 Hz. It is quite easy to analyze free vibration in FEA, however, experimentally it is not feasible to provide for a truly free support – the structure must be held in some way. A good approximation, though, would be to suspend the toolholder from two long strings. Figure 17 illustrates the experimental setup of the toolholder. Strings approximately 2 m long were attached to the retention stud and to the tool. Long strings are needed to ensure very little local stiffening at the point of attachment. A good suspension support is achieved if the rigid body modes, while no longer have a zero natural frequency, have values that are 10-20% that of the first bending mode. This is to ensure that the rigid body modes do not significantly influence the flexural modes that are the object of the test.

Under ideal conditions and to achieve the best results, the accelerometer should be firmly attached to a flat surface on the test object. However, since the toolholder is

cylindrical. flats would need to ground at numerous locations. This needs to be avoided since the flats will cause an unbalance, rendering the toolholder useless for machining. Good results are achieved, though, by using an accelerometer with a very small base. Minimizing the space between the toolholder's curvature and the base will reduce any noise error.

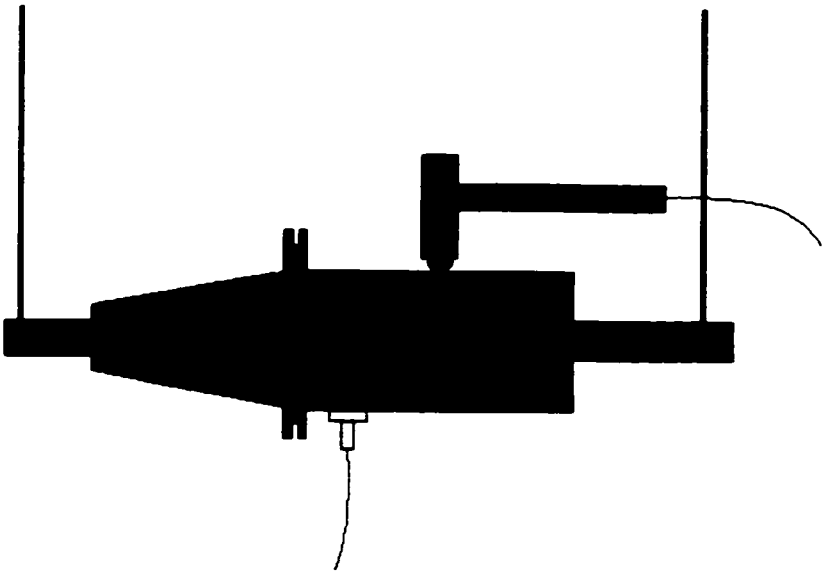

Figure 17 – Setup for Free Vibration Testing

The use of contact cement or a tapped hole are preferred methods of firmly securing the base onto the structure. However, these methods are permanent and, since the toolholders will be used later for machining tests, the accelerometer is attached using a thin layer of wax. It is important, though, to use a minimal amount of wax, as too much will affect the results by damping the vibration.

Testing was done using a Hewlett Packard 35660A dual channel dynamic signal analyzer. A PCB accelerometer (model 303 A02) was used and rated for a frequency range of 1 to 10000 Hz. It had a base diameter of 5 mm. The impact hammer had a

rounded steel tip and no added mass. It used a PCB force transducer (model 086 B01). Both were connected to PCB signal amplifiers (model 480 D06). The analyzer was set to perform a frequency response analysis with the hammer set as the trigger on the first channel and the accelerometer set on the second. It was determined through preliminary testing that the response signal decayed well before the end of the record length and the force signal was adequately noise free. Thus, no windowing functions were needed on either channel.

Two CAT 40 (V-flange) toolholders of different lengths (see Figure 18) were selected for testing. The CAT designation is short for Caterpillar, the company which developed the V-flange system (standardizing the way the toolholder was gripped by automatic tool changers) and the 40 represents the maximum taper diameter (in millimeters) of the shank.

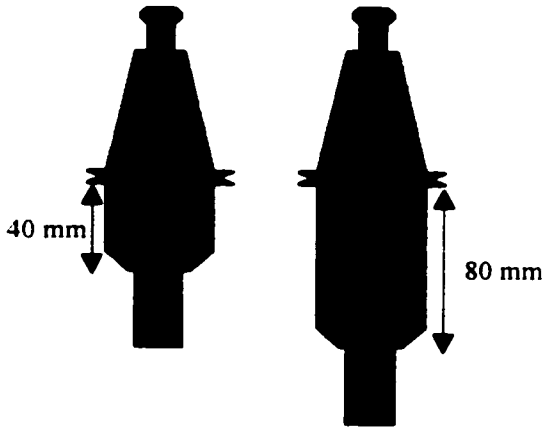

Figure 18 – Sizes of CAT 40 Toolholders used for

Testing involved impacting the toolholder five times in the same location to average out noise or bad hits in the FRF. This procedure is repeated many times with either the impacting occurring at different locations or the accelerometer mounted at different

locations. This is not done to acquire the mode shapes, which involves testing at various locations, but rather to check accuracy and consistency of the results. If the accelerometer happened to be mounted on a nodal point, a particular mode might not appear clearly on the FRF.

Before accepting the results, the quality of the measurements needs to be checked. A good indicator is the coherence function. Coherence is a statistical concept that relates how well the output of the structure is related to the input to the structure. It is calculated at every frequency ω and is rated on a 0 to 1 scale (0 being pure noise, 1 for no noise contamination). In practice, data with a coherence of less than .75 would indicate that the test should be redone. Note that since the coherence function is based on statistical averages, coherence for a single measurement would be unity. Only after several measurements are averaged can the coherence function detect the lack of relationship between the output and input signals. The primary reason for low coherence values is noise from cables, amplifiers, transducers, A/D converters, and so on. At frequencies of low structural response, the effects of noise become more apparent as the signal-to-noise ratio decreases (response signal will be at a low level, but noise level remains the same). Since noise is constantly fluctuating, low values of coherence often result at anti-resonance frequencies. Another possible source of low coherence is variations in impact force. Since coherence is an averaging technique, differences in the force at each impact will produce a 'noisy' effect in the coherence plot. Therefore, it is important to consistently strike the object with the same force.

Once a good FRF plot is generated the last step would be to verify that the peaks of the frequency response are actually natural frequencies. This is done by checking the real

and imaginary parts of the frequency response. For a proportionally damped system, the imaginary part is maximum or minimum at resonance and the real part is zero.

The experimental results for the short toolholder are shown in Figures 19(a) through 19(c). The frequency response is shown in (a), the real and imaginary components are shown in (b), while the coherence plot is in (c). Similarly, the results for the long toolholder are shown in Figures 20(a) through 20(c). Tables 2 and 3 summarize the results for the long and short toolholders, respectively, against those found through FEA. In both cases, the greatest variation was in the first mode, but the next two modes were quite close. Errors from both methods can account for the differences. The finite element model had small simplifications and some of the internal geometry could not be measured directly and had to be estimated. Also, solid mesh elements tend to be stiffer which would result in higher frequency values being obtained. On the experimental side, many errors are likely to occur. The use of strings to suspend the toolholders, noise in the instruments, improper impacting techniques and a host of other variables can all contribute to error. Another contributing factor may come from a required assumption that was made in the finite element model. Recall that since the software package cannot model any looseness between assembled components, it was assumed that the components of the toolholder (retention stud, set screw, tool) were rigidly in place. In effect, the toolholder would behave as though it was a single piece of steel. In such a case, FEA would report higher frequencies. In actuality, there may be looseness between

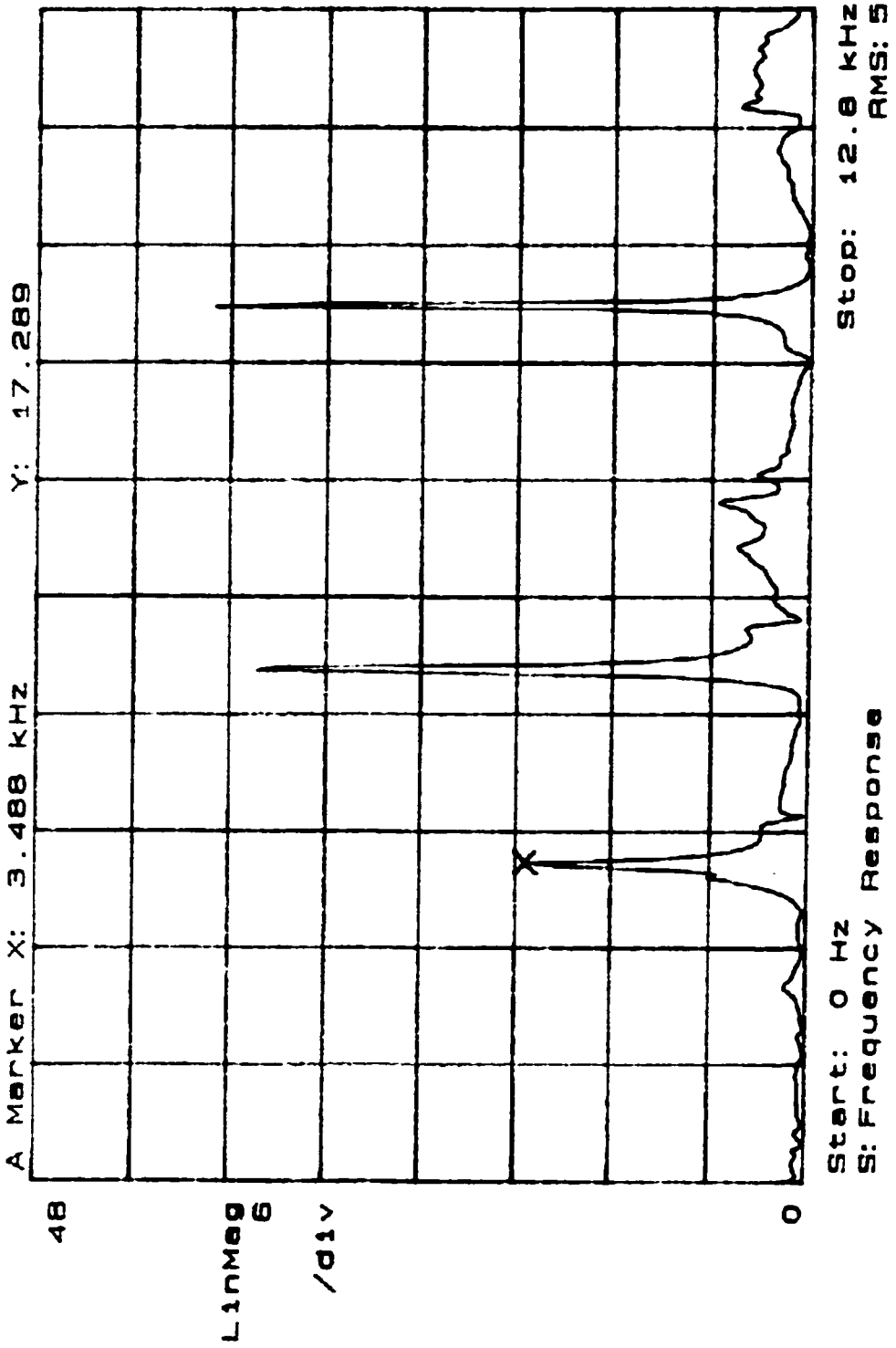

Figure 19a – FRF of Short Tapered Toolholder

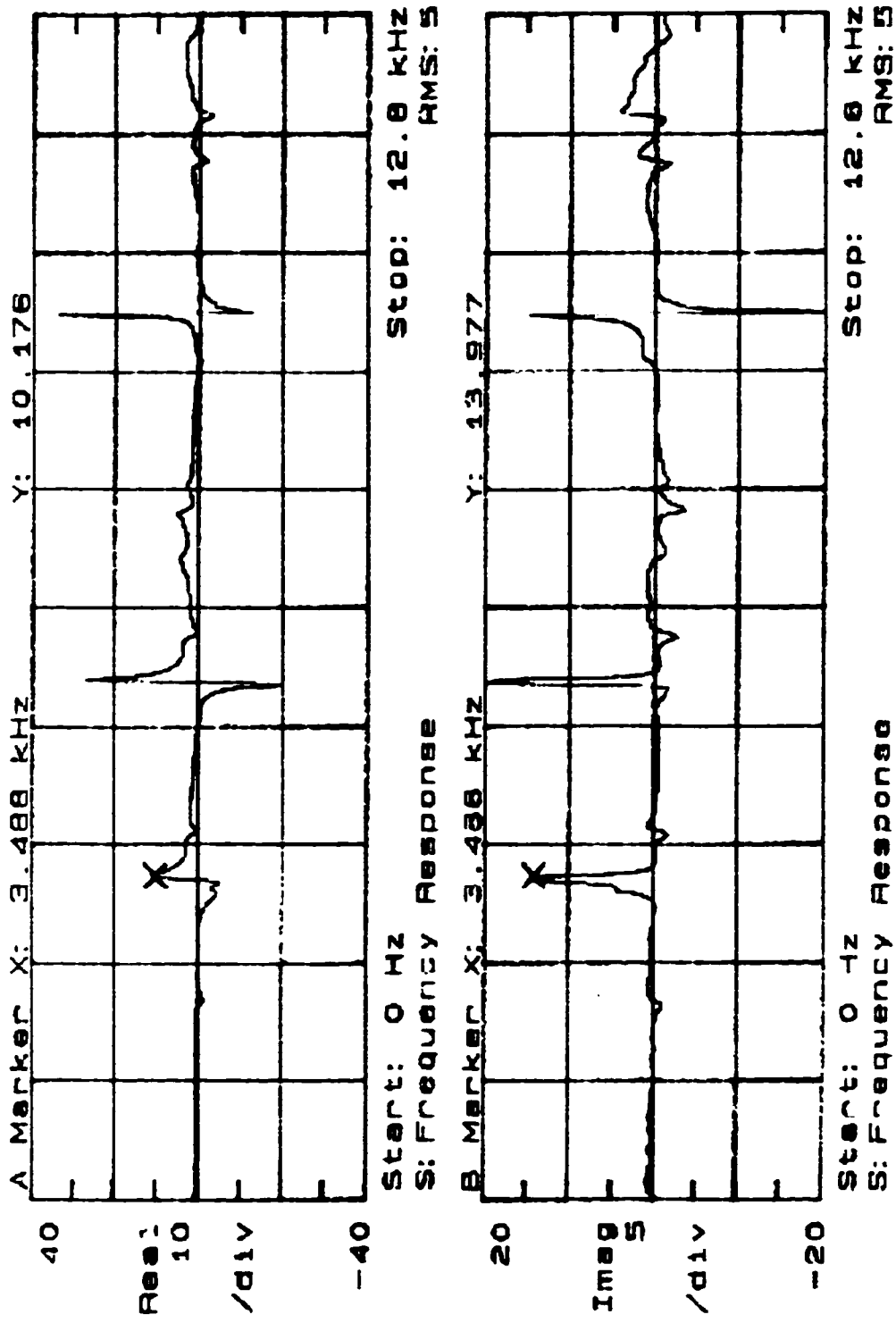

Figure 19b – Real and Imaginary Parts of FRF

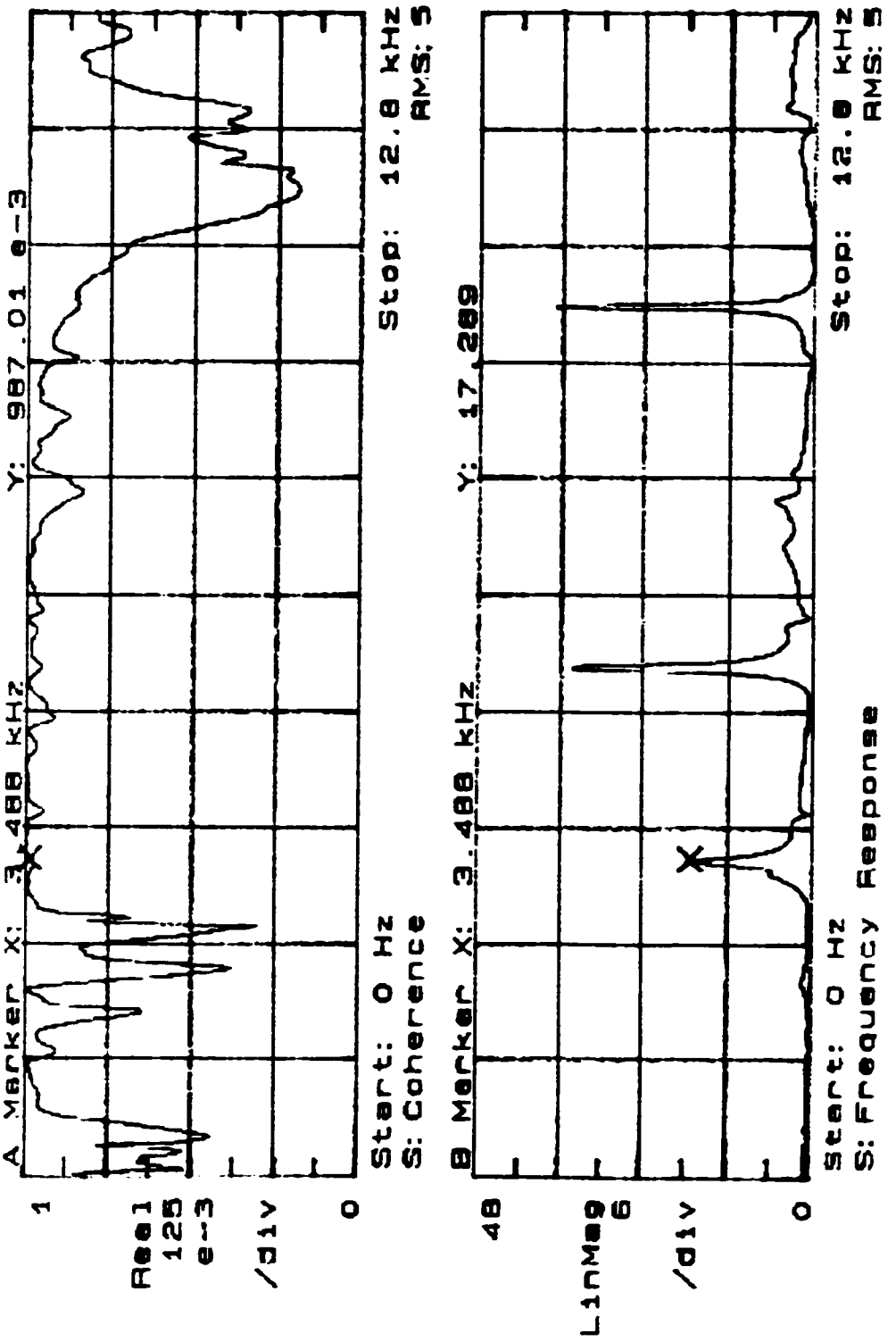

Figure 19c – Coherence Plot for FRF

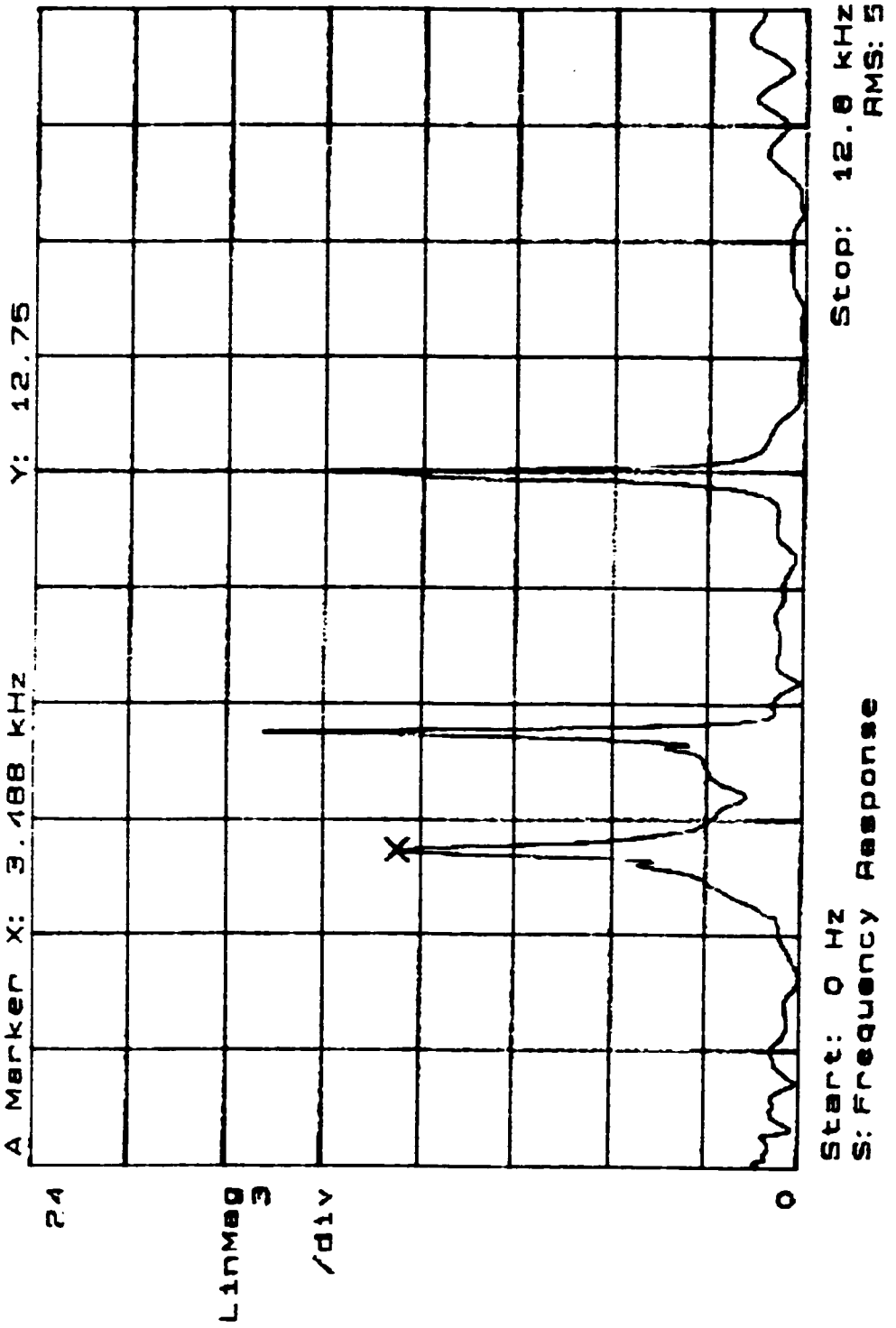

Figure 20a – FRF of Long Tapered Toolholder

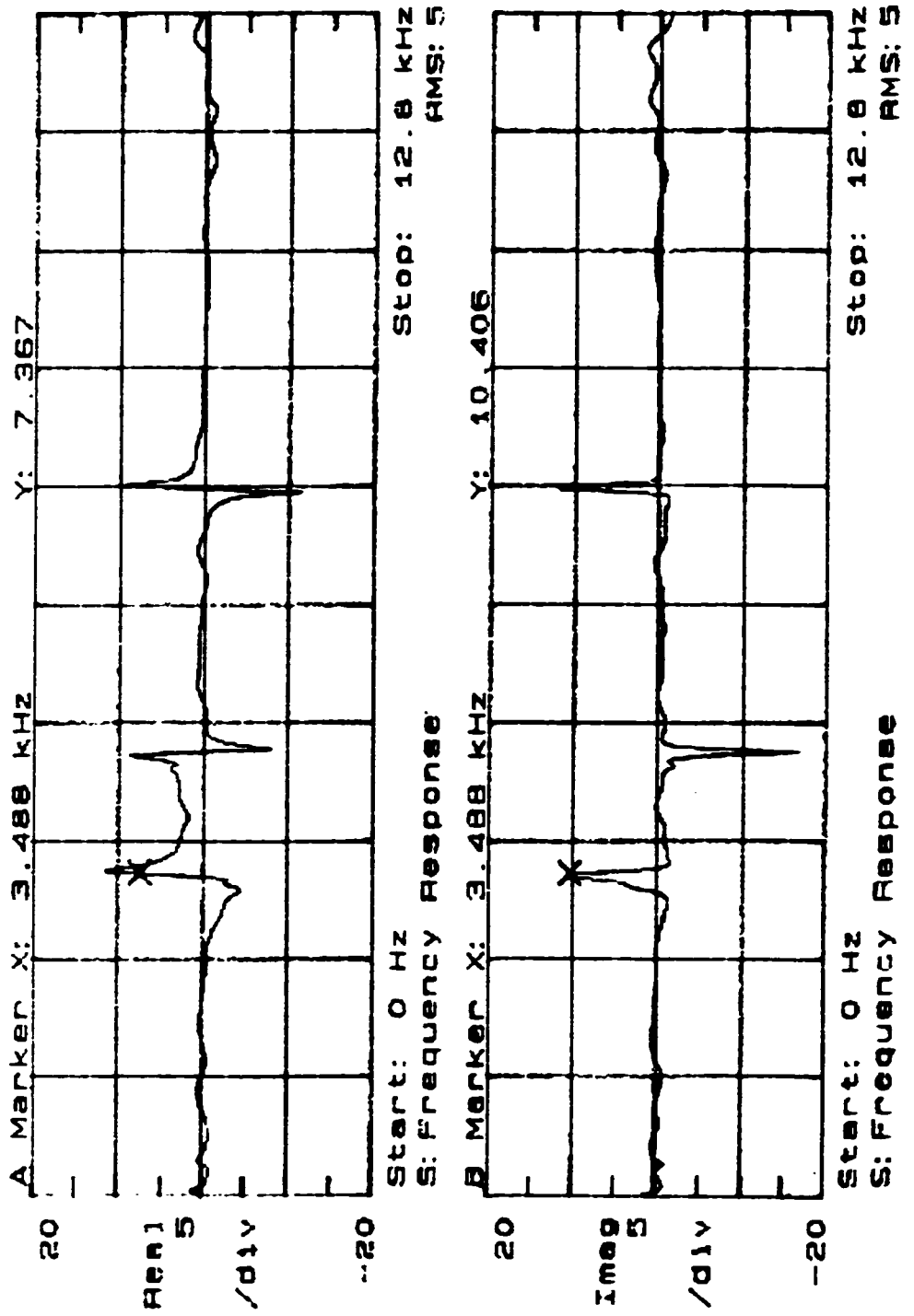

Figure 20b – Real and Imaginary Parts of FRF

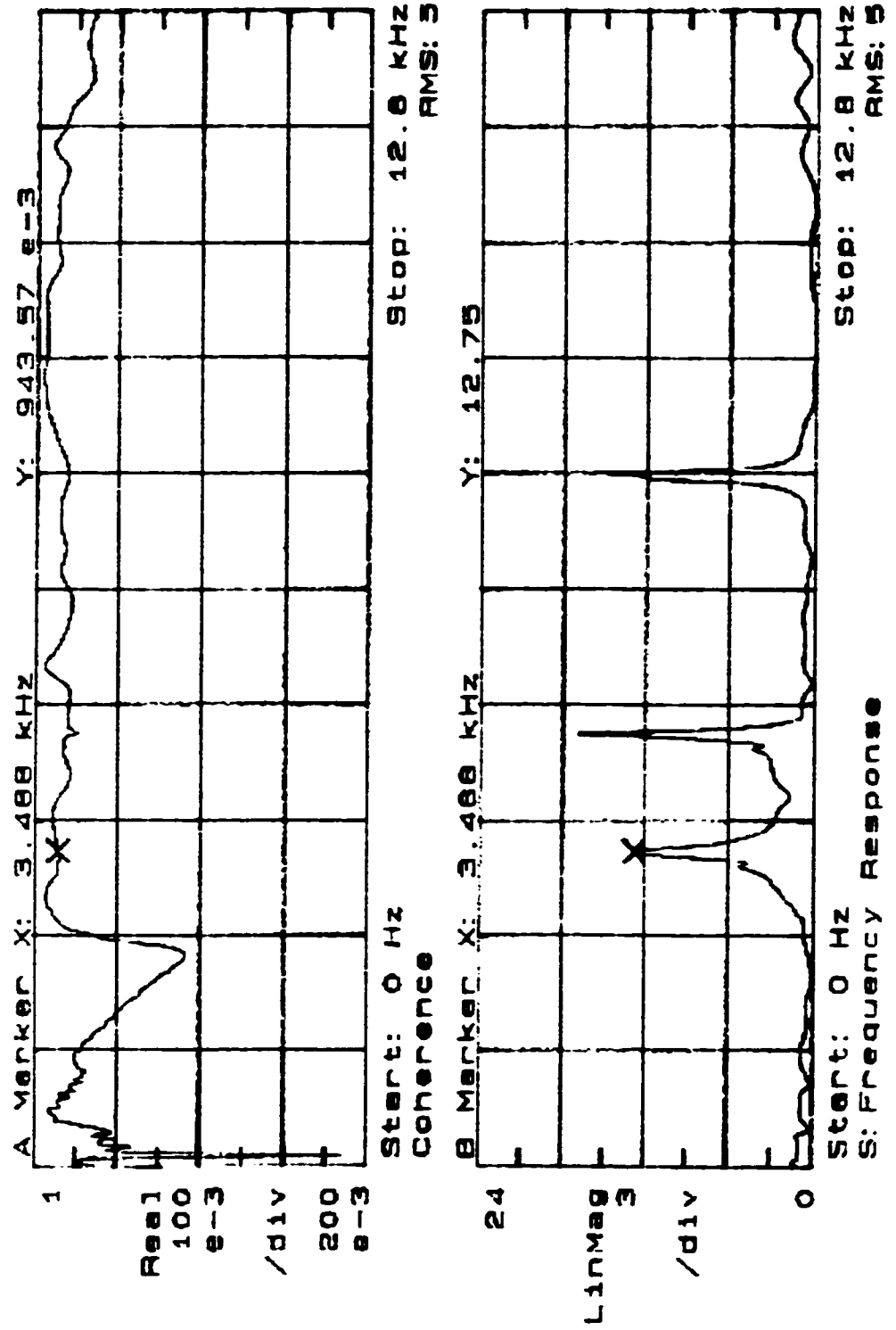

Figure 20c – Coherence Plot for FRF

the components, which experimental testing would pick up, resulting in lower frequencies.

Mode	FEA Results (Hz)	Exp. Results (Hz)	% Difference
1	4122	3488	15
2	5165	4832	6
3	7696	7648	1

Table 2 - Verification of a Long Toolholder

Mode	FEA Results (Hz)	Exp. Results (Hz)	% Difference
1	4374	3488	20
2	5413	5600	4
3	8915	9568	7

Table 3 - Verification of a Short Toolholder

Unfortunately, there is not much that can be done to improve the results since there are limits to what FEA can do. Recall, also, that reducing the mesh size made very little difference. However, taking into account all the possible sources of error, the results are quite acceptable.

C. Application of Boundary Conditions

Boundary conditions create enforced environmental conditions on a finite element model. There are various types of boundary conditions (displacement, temperature, heat load), but in a vibration analysis, displacement restraints are usually the only type used. Displacement restraints are known displacements and rotations applied to nodes (or surfaces, edges) that limit one or more degrees of freedom.

One of the most important steps in preparing for an analysis is to apply boundary conditions that accurately reflect the environment that the part will see in operation. It

was previously mentioned that an inadequate mesh could yield bad results, but through continuous refinement the solver would converge on the correct result (assuming everything else is correct). However, if the wrong boundary conditions are applied, no amount of mesh adjustment will improve the model; the solver will simply converge on the wrong result. Even slight modifications to the boundary conditions could significantly change the final results.

Before getting into more detail about the application of the boundary conditions, a decision needs to be made on how to handle the spindle. The fretting condition occurs because of the relative displacement of the toolholder and spindle surfaces. Since the cutting forces are applied to the toolholder, it is obvious that its deflections need to be studied, but would it necessary to model the spindle as well? It would be advantageous to leave the spindle out of the analysis since its inclusion would make the finite element model very large and complicated. It would become a much more difficult task of modeling the many different spindle designs and configurations that exist. The spindle and the contribution it makes to the fretting condition needs to be examined closely.

A spindle is a motor-driven shaft that both positions and transmits torque to the toolholder, so its precision is crucial to the machining operation. The key factor affecting this precision is the spindle's bearings. From one to three sets of bearings commonly support each end of a spindle shaft. Common bearing types include ball bearings, roller bearings and tapered roller bearings; each being stiffer than the previous. The main goal in designing a spindle is to reduce its deflection. A rule of thumb is that shaft deflections account for 50-70% of the total spindle deflection, while the bearings are responsible for

between 30-50% [3]. Whether the spindle's deflections are significant (and contribute to the fretting problem) needs to be decided.

Modal analysis was done on a Cincinnati Milacron Arrow 500 vertical machining center. The goal of the testing was to determine the spindle's first mode of vibration. If well designed, the natural frequency should be well above normal operating speeds to prevent vibration problems. Since the spindle is located within a housing, it would have been very difficult to gain access to perform the many tests needed along its length. The numerous tests are required to get an accurate portrayal of its dynamic response. As it was, less than one inch of the spindle was exposed for testing. However, this should be sufficient to get a general idea of its dynamic behaviour. The tests were performed in the same manner as was done with the toolholders; mounting the accelerometer using a thin layer of wax and impacting multiple times to average out noise error. The frequency response of the spindle is shown in Figure 21. The first mode is approximately 350 Hz which translates to a spindle speed of 21000 rpm. Normal operating speeds for this machine are less than 3000 rpm or 1/7 that of the first natural frequency. At this point, it would be a fair assumption to say that the spindle would behave as a rigid body at the lower typical operating frequencies. With this assumption, the spindle does not need to be modeled.

However, a better reasoning exists that does not require modal analysis, but just a keen observation. When the toolholder is in the spindle, it becomes a component of the spindle assembly and is fixed only within the spindle. If the spindle deflects, the toolholder will move with the spindle. However, there would be no relative displacement between the spindle and the shank of the toolholder; a requirement for fretting to occur.

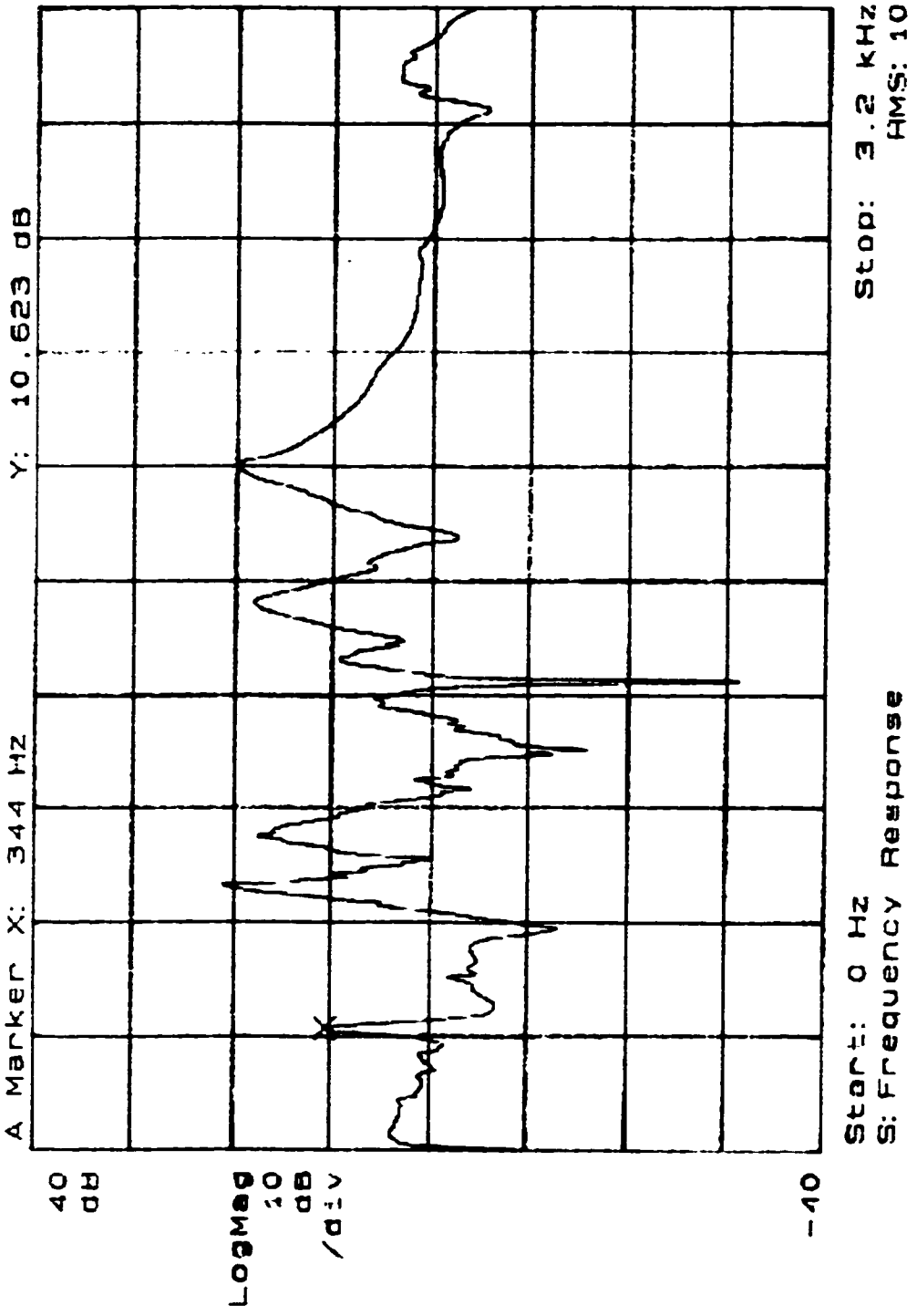

Figure 21 – FRF of Spindle

In fact, there is no way that the spindle, itself, can deflect and cause impact with the toolholder shank. Impacting can only occur when the toolholder flexes. Therefore, relative to the toolholder, the spindle can be seen as being fixed and, therefore, ignored in the finite element analysis. Referring to Figure 22, four possible cases can occur. In (a), neither the spindle nor the toolholder have deflected. In (b), the toolholder deflects, but not the spindle. In (c), the spindle deflects, but not the toolholder. Finally, in (d), both spindle and toolholder deflect. Notice that in (a) and (c) there is no relative displacement (and no fretting) between the shank and the spindle, although the spindle has deflected in (c). Figures (b) and (d) are also identical in that fretting will occur regardless of whether

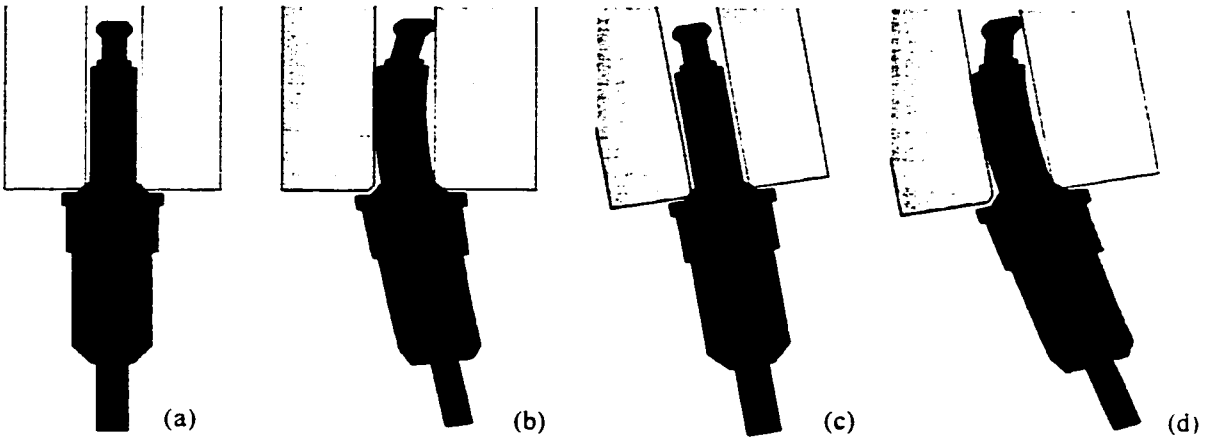

Figure 22 – Possible Spindle/Toolholder Deflections

the spindle deflects. It can then be concluded that fretting depends only on whether the toolholder deflects.

Now that it has been shown that the spindle can be ignored, the next step is the application of boundary conditions to the toolholder models. Two different types of toolholders will be studied at this point: tapered shank and straight shank. As previously

discussed, mesh verification testing was done on tapered shank (CAT 40) toolholders. Unfortunately, no testing was done on straight shank toolholders because of their unavailability. In spite of this, the mesh type and density that was used with the tapered shank toolholders should yield results with comparable accuracy for the straight shank toolholders.

Figure 23 illustrates how the two toolholder designs sit within the spindle pocket. What needs to be decided is what type of displacement restraints are required and where

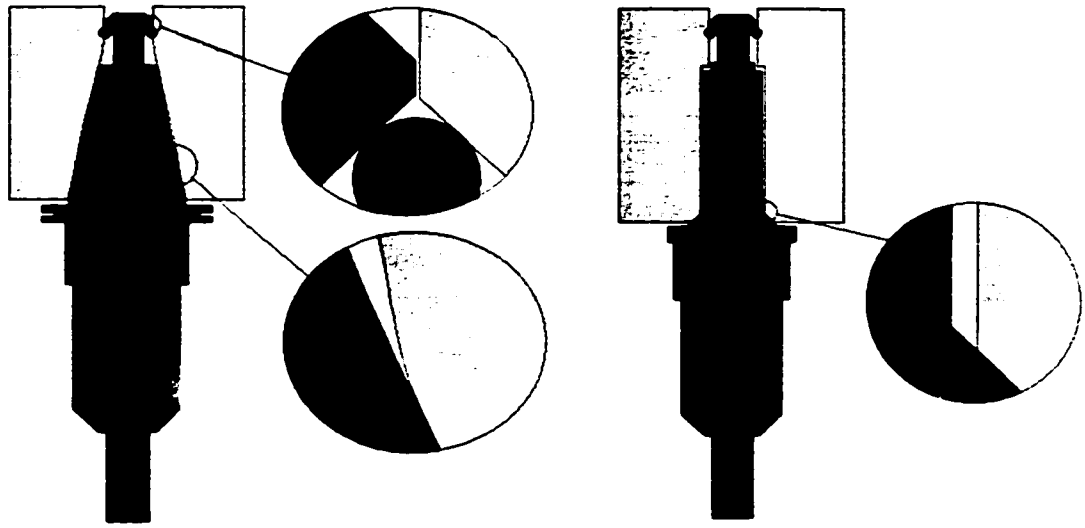

Figure 23 – Key Features in Toolholder/Spindle Interface

they should be applied. Both designs have a retention stud which is held tightly by a clamping mechanism. This mechanism also servers to pull the toolholder's external taper firmly against the spindle's internal taper. The tapered shank toolholder has two areas (or bands) of its taper which come into direct contact with the spindle. These areas provide for the actual alignment of the toolholder and are located near the bottom and top portions of the shank. The straight shank toolholder has a taper that is separate from the

shank. Referred to as an alignment taper, it has a smaller area of contact than the other design. The extra contact in the tapered shank design allows for greater precision in alignment and reduces of the chances of the toolholder shifting during operation.

Since the toolholder taper is held tightly against the spindle taper, it is certainly restrained laterally, as well as from any upward movement (into the spindle), but there may be some downward movement. During cutting, particularly milling, the toolholder will bend resulting in its taper slipping out slightly on one side (see Figure 24). Although the alignment taper restricts the toolholder from moving upward, there is nothing to prevent it from sliding out (even if it is a very small displacement). Since restraints can only be placed on known conditions, the tapered areas of the toolholders will be fixed laterally, but will be free to move vertically.

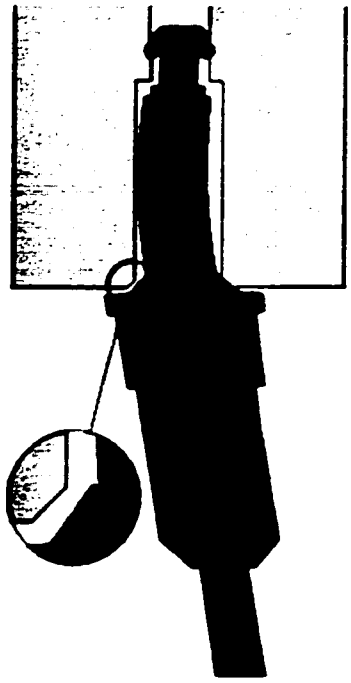

Figure 24 – Illustration of how Alignment Taper can Slip out of Spindle Taper

The clamping mechanism in the Milacron 500 is shown in Figure 25. When the toolholder is inserted into the spindle and the mechanism activated, four steel balls push

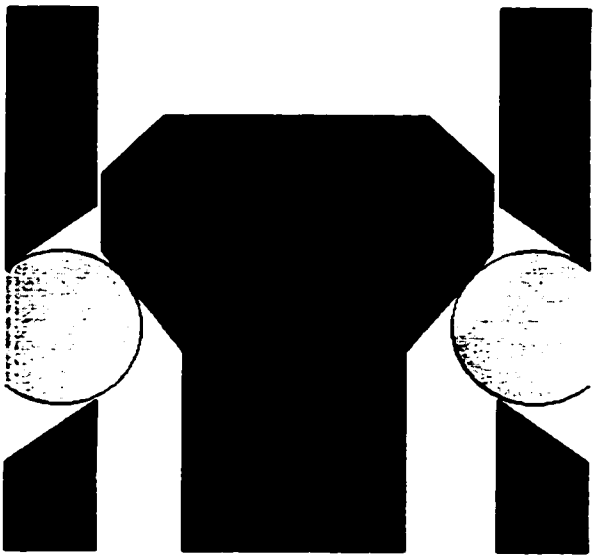

Figure 25 – Illustration of Clamping Mechanism

against the bottom taper of the stud pulling the toolholder up into the spindle. It will be assumed that the steel balls lock tightly in place so as to prevent the stud taper from moving laterally and downwards, although there is nothing restricting it from moving upwards. This was just the opposite situation with the alignment taper which could move down but not up. However, vertical restraints need to be applied to the retention stud to fix the model in space. During machining, the flexing of the toolholder may cause the alignment taper to slip out of its pocket so it was left unrestrained. There is, however, no possible way for the toolholder to be pushed further up into the spindle pocket and the steel balls prevent stud from moving downward (assumed). Therefore, it is reasonable to assume that the stud taper will not move in any direction and restraints can be applied in

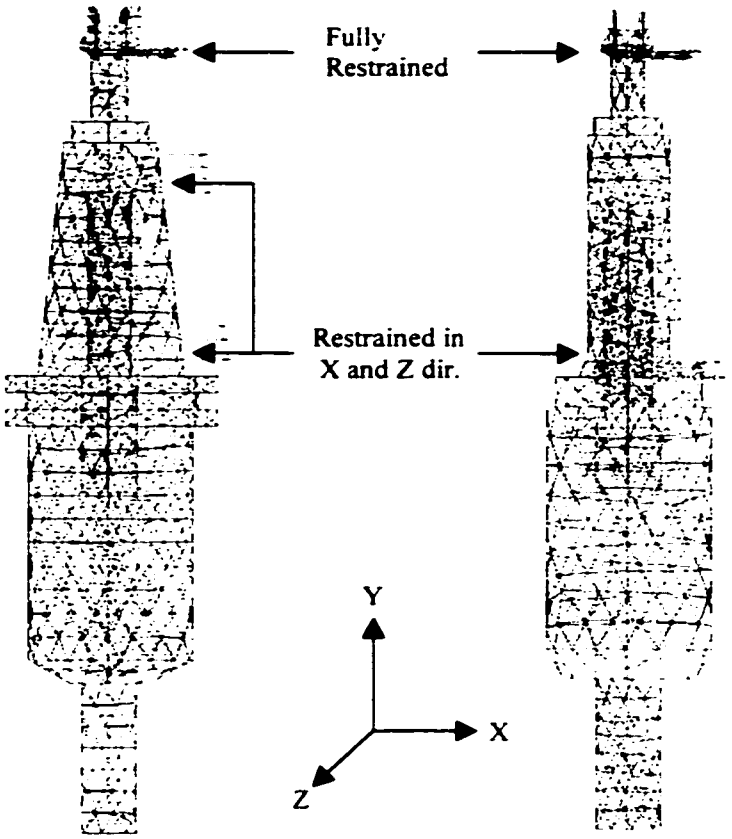

Figure 26 – Meshed Models with Boundary Conditions

all three directions (X,Y,Z). The meshed models with the applied boundary conditions are shown in Figure 26.

D. Results

Once a finite element model has been completed, it can be analyzed using the solver within I-DEAS. The solver was set to perform a normal mode dynamic analysis, which can use several different formulations to obtain the natural frequencies and mode shapes. These formulations include the Lanczos method, Guyan method and the Simultaneous Vector Iteration (SVI) method. The Lanczos computational method is generally more efficient and was used for the analyses. The mass lumping option was also activated in

the solver. For structural vibration problems, mass lumping "softens" the discretized model, which can improve the accuracy of the results. Detailed information about the different computational methods, as well as mass lumping, are available in the I-DEAS help files and in many FEA books.

Many toolholder designs were studied with varying lengths and diameters. Tables 4 and 5 summarize the natural frequencies of the first three modes for the tapered and straight shank toolholders, respectively. Refer to back Figure 14 for an explanation of dimensions. The shank length of all the toolholders is identical at 70 mm.

Body Length (mm)	40	80
Body Diameter (mm)	45	45
Mode	Frequency (Hz)	
1	2164	1443
2	2995	2805
3	4997	4656

Table 4 - Results for Tapered Shank Toolholder Designs

Body Length (mm)	40	80	120	80
Body Diameter (mm)	45	45	45	65
Mode	Frequency (Hz)			
1	1324	720	460	510
2	2930	2350	2010	1620
3	5140	4825	4220	4793

Table 5 - Results for Straight Shank Toolholder Designs

Note that the two tapered toolholders analyzed here are the same ones used for the experimental free vibration testing, while the straight shank models do not necessarily represent actual toolholder designs.

Examination of the results yields the following conclusions:

1) Tapered toolholders have higher natural frequencies than those of the straight shank design indicating greater stiffness
2) Increasing the length results in lower natural frequencies indicating lower stiffness
3) Increasing the diameter results in lower natural frequencies due to an increase in mass

Although the trends in the results are not surprising, it is interesting to see how the natural frequencies are affected by the design changes. For example, examine the differences in the first and second modes of the straight shank model. From a length of 40 to 80 mm the frequency drops by about 600 Hz and from 80 mm to 120 mm the drop is about 300 Hz. However, in the third mode the reverse is true; from 40 to 80 mm the drop is 300 Hz, while from 80 to 120 mm the drop is 600 Hz. Also, examine the straight shank models with the same lengths, but different diameters. The increase in mass makes significant differences in the first two modes, but virtually no difference in the third. The point is that, although general trends in the results can be hypothesized, simulations need to be done to confirm, not only changes to the results, but more importantly, the magnitude of the changes.

The first mode shape is shown in Figure 27 for the straight shank toolholder. If the deflection of the shank is great enough to impact the spindle wall, a fretting condition will exist. However, knowing only the natural frequencies and mode shapes is not sufficient in determining the magnitude of the deflection. In order to calculate actual shank displacements, simulated cutting forces need to be applied to the model.

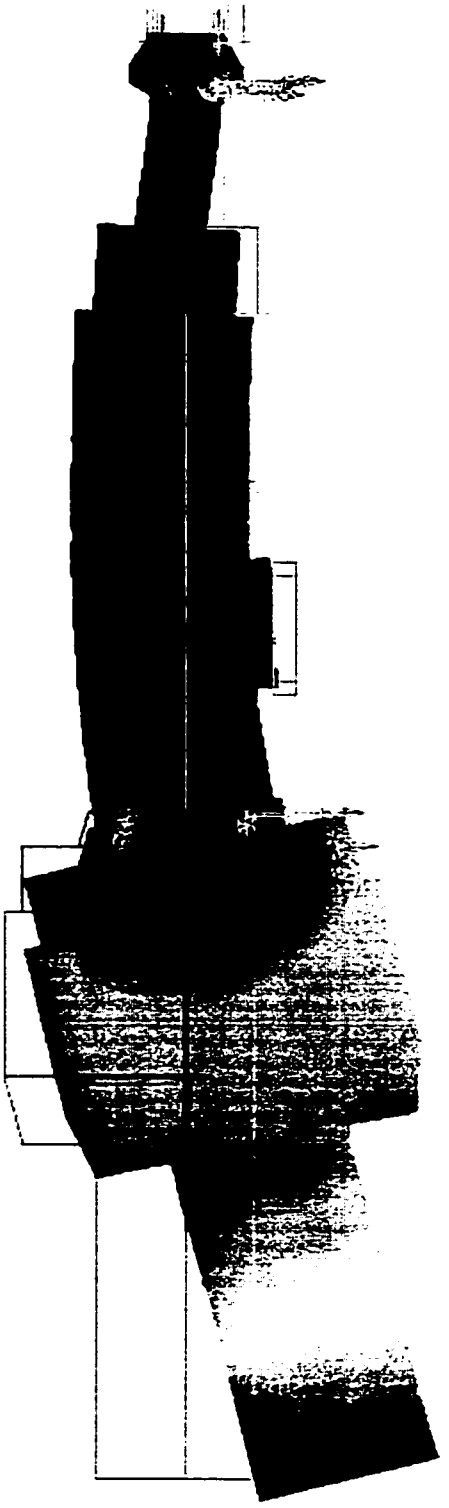

Figure 27 – First Mode Shape of Straight Shank Toolholder

V. Response Prediction

A major design goal of many engineering analyses is predicting physical responses to actual operating forces. The I-DEAS Model Response software is a tool that performs such a task by evaluating the responses of a dynamic model under applied excitations. A dynamic model is a finite element model with a set of normal modes (obtained from normal mode dynamic analysis).

A. Defining Excitations

There are basically two types of machining processes based on the tool's movement relative to the work piece. In a drilling process, the tool's movement is perpendicular to the surface of the work piece. In such a case, there is little or no bending of the toolholder. Referring to Figure 28a, all the teeth on the tool are in continuous contact with the material so the resultant forces in the X and Y directions are zero. The thrust force will not contribute to the bending of the toolholder. In a milling process the tool moves across the surface of the work piece. In Figure 28b, it can be seen that not all teeth are in contact with the material so the resultant force is not zero. It is the resultant force that will cause the toolholder to bend during operation. It is, therefore, only important to study milling, since it is the only machining process that would cause the toolholder to bend.

Excitations can be defined in one of several ways. Forcing functions, in either the time or frequency domain, can be applied to one or more nodes in the model. Rotating forces, which do not vary with frequency, and unbalance forces, which do vary with

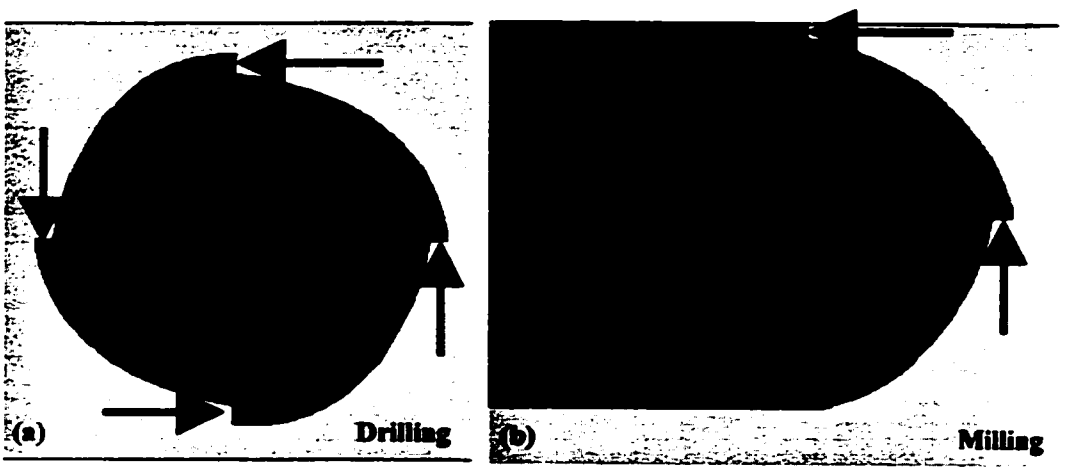

Figure 28 – Cutting Forces on Tool Teeth

frequency, can also be applied to nodes. Also, forces can only be applied to unrestrained degrees of freedom.

The goal of this work is to obtain frequency response functions and, later, displacement responses. Achieving this requires working in the frequency domain. This means that the forcing function that will simulate cutting will have to be specified as a function of frequency. There are two ways to do this. The first requires entering the magnitude of the force at each frequency. For example, if a force with a sinusoidal waveform has a magnitude of X with a frequency of Y in the time domain, then the force would be a single line of length X at the frequency Y as shown in Figure 29. This function has only one magnitude at one operating frequency, however, typical cutting forces are not so simple and their content contains many different magnitudes, each at a different operating frequency. It, therefore, becomes less intuitive to specify the forcing function directly in the frequency domain. The solution would be to use the second method of specifying the force in the time domain (which would be much easier to visualize and understand) and then performing a forward Fast Fourier Transform (FFT) to

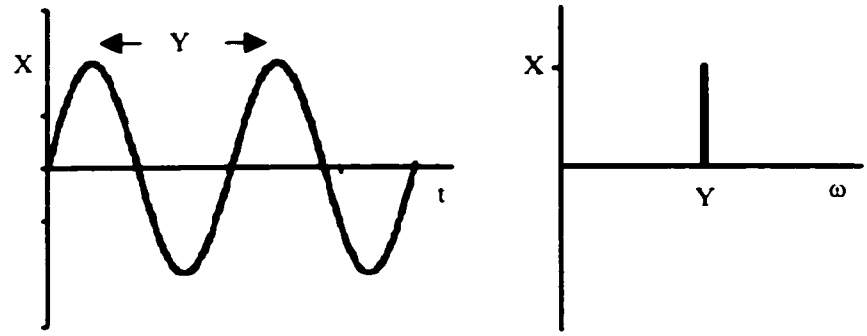

Figure 29 – Sinusoidal Waveform in Frequency Domain

convert the force in the time domain to the frequency domain. Figure 30 shows an example of this.

After specifying the forcing function and calculating the FRF, the displacement response can be found using the following relation:

$$X(\omega) = H(\omega) \cdot F(\omega) \tag{1}$$

where

X = displacement as a function of ω
H = frequency response function in terms of compliance (displacement/force)
F = applied force as a function of ω

The displacement response (see Figure 31) shows the displacements of the structure at each frequency were a force occurs. But what would the displacements be if the forces were at different frequencies or if the magnitude of the forces were different? In order to find out, a new forcing function would have to be created in the frequency domain with the new magnitudes applied at the new frequencies. Then, a new displacement response would be calculated. However, to facilitate the comparison of displacement responses between different toolholder designs and to avoid creating new forcing functions to cover all frequencies of interest, a single force magnitude could be specified over the entire

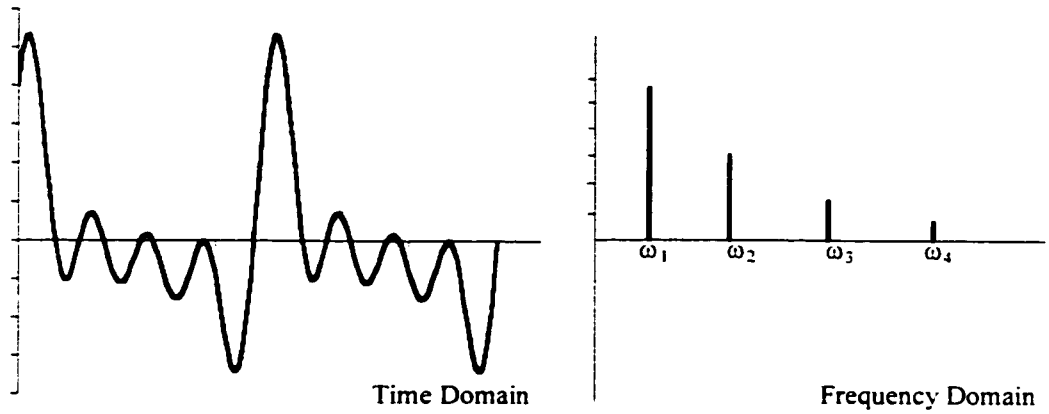

Figure 30 – Complex Function in Frequency Domain

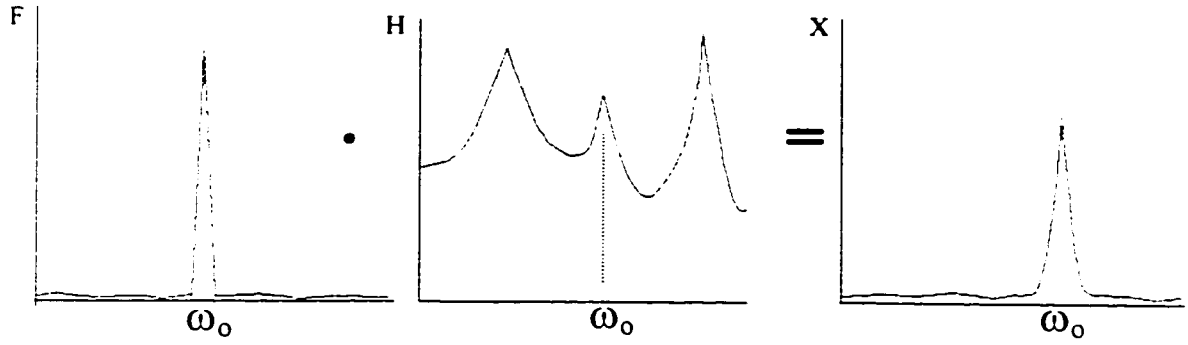

Figure 31 – Displacement Calculation

frequency range. In effect, the force function F(ω), in equation (1), is being replaced with a constant which will simply re-scale the FRF. The result is a plot that will indicate the physical displacement under a given load at any frequency. An example is shown in Figure 32.

B. Calculation of Damping

Before the displacement response can be found, damping ratios need to be specified. Damping in a structure controls the decay of vibrations. If the structure is lightly damped, it will vibrate for a greater duration than one that is heavily damped. The

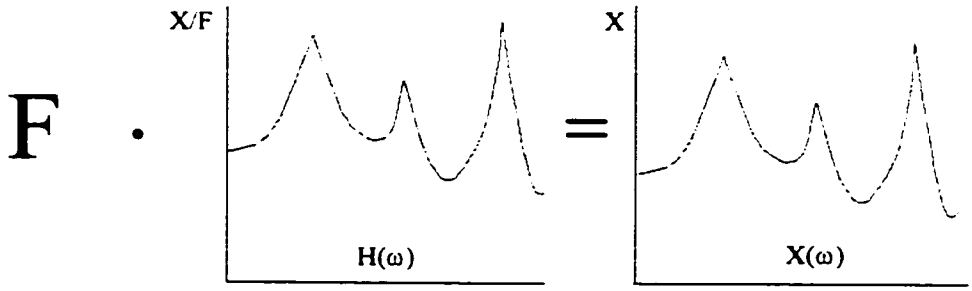

Figure 32 – Displacement Calculation from Constant Force

effects of damping can be viewed in a FRF. Sharp, narrow peaks indicate a lightly damped structure while flatter, wider peaks are typical of heavily damped structures. The calculation of the damping ratios was performed using experimental modal testing on the toolholders in the free vibration state. Once a FRF is generated, the –3 dB bandwidths of the peaks or the 'half-power points' need to be found. Because the peaks on lightly damped structures are too narrow for accurate measurement, zoom analysis is used to obtain sufficient frequency resolution for the measurements.

Figure 33 is a frequency response function of the long tapered toolholder showing only the first mode. The FRF of this toolholder was previously shown (in mesh verification) with a scale of 6400 Hz. With the analyzer capable of plotting only 400 points, each point on the plot represented 16 Hz. However, by zooming in on a peak to a minimum span of 800 Hz, each point now represents 2 Hz; an increase of resolution of eight times. The damping ratio can now be accurately obtained using the following formula.

$$\zeta = \frac{\omega_b - \omega_a}{2\omega_d} \qquad (2)$$

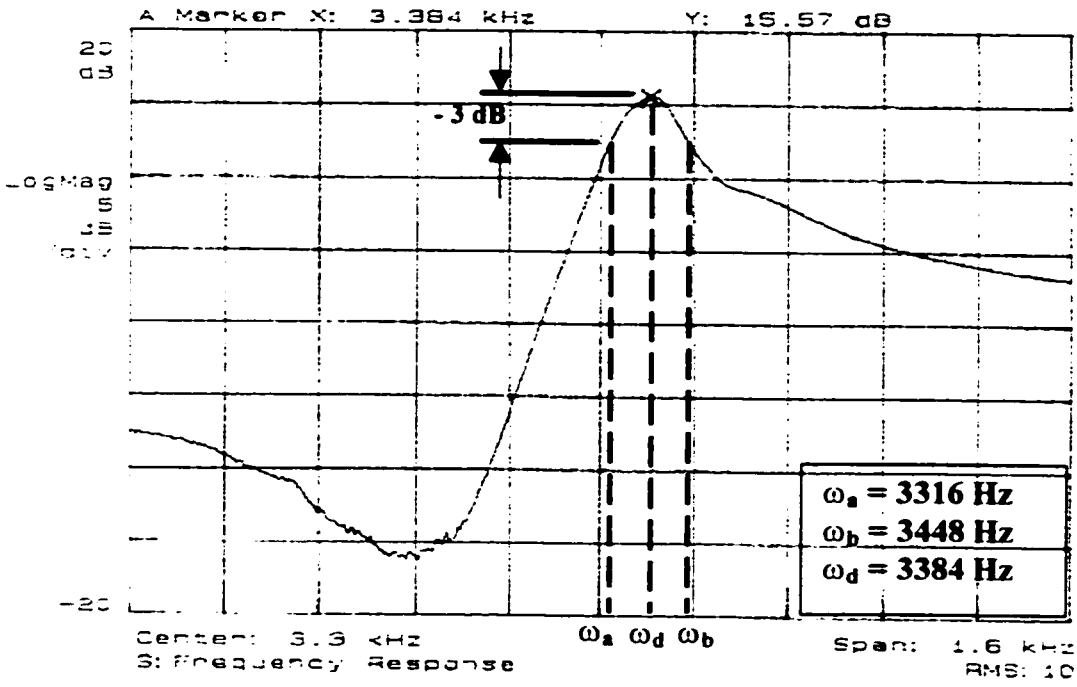

Figure 33 – Damping Coefficient Calculation

For this particular mode, the damping ratio was approximately .02. Other modes had similar or slightly less values. For simplicity, the same damping ratio of .02 will be used for all modes in each analysis. The same damping ratio will be used for the straight shank toolholders, which could not be tested experimentally.

C. Results

At this point, simulated cutting forces can be applied to the model. In milling operations, the magnitude of the cutting force is typically around 500 N and could go as high as 1000 N or more under heavy cutting. These two forces were applied (individually) to all the models at the tool tip. Displacements were then calculated at three nodes evenly spaced along one side of the shank as shown in Figure 34. Once the plots have been generated, displacements can be found at any operating frequency. The operating frequency is the frequency at which the force is applied to the structure and, in

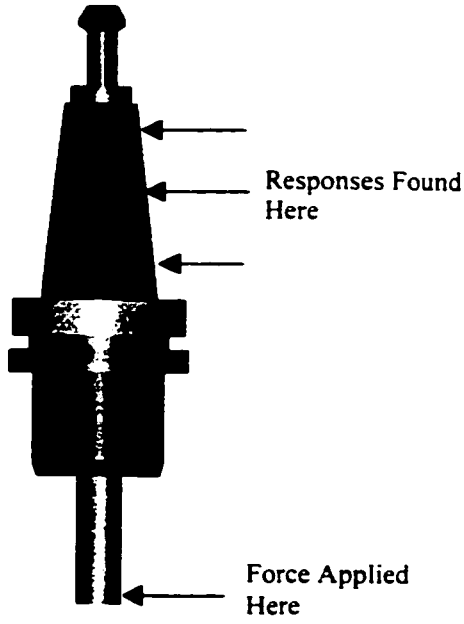

Figure 34 – Locations of Force Application and Response Calculation

the case of a toolholder, is the cutting frequency. It is calculated by multiplying the spindle speed (converted to Hertz) by the number of teeth on the tool. For example, a spindle speed of 3000 rpm (50 Hz) with a four tooth cutter results in an operating frequency of 200 Hz. The shank displacements for the six toolholder models (four straight shank, two tapered shank) are shown in Table 6 for an operating frequency of 200 Hz.

Force (N)	Straight Shank				Tapered Shank	
	Short L=40 mm	Medium L=80 mm	Long L=120 mm	Wide D=65 mm	Short L=40 mm	Long L=80 mm
500	.0072	.0079	.012	.008	.00045	.0007
1000	.011	.016	.023	.017	.001	.0013
L = Length of Body D = Diameter of Body All Displacements in Millimeters (mm)						

Table 6 - Shank Deflections Under Given Load

The frequency responses are shown in Figures 35 to 40. Only the first mode is shown for each case because operating frequencies are typically low and rarely get as high as the first resonance. At 0 Hz there is an initial displacement corresponding to the static deflection of the shank under the applied force.

There is an important observation that can be made about the frequency response functions. At low frequencies the response is dominated by the stiffness of the toolholder. If the toolholder has a high first resonance, indicating high stiffness, the frequency response function has a longer 'flat' section (low slope) at the start. As the stiffness decreases the resonance peak shifts to the left and there is less of a 'flat' section. Compare Figures 35 and 37, which illustrate this point with the short and long straight shank toolholder. With the short toolholder, the frequency reaches approximately 500 Hz

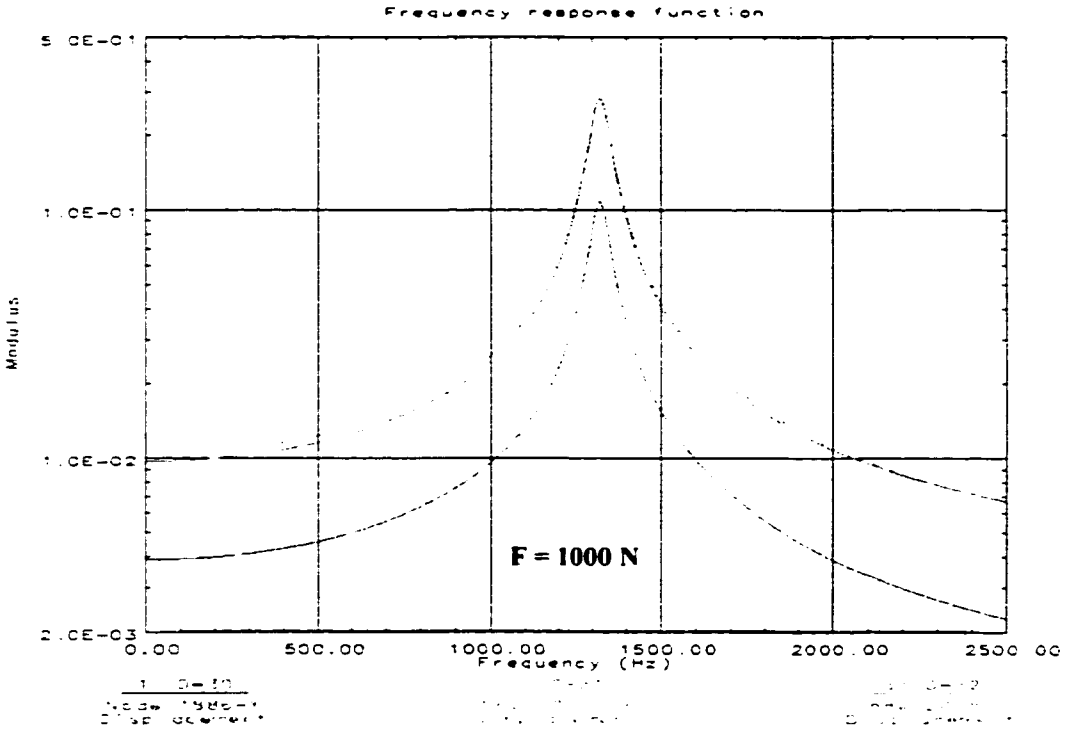

Figure 35 – Displacement Response for Short Length Straight Shank Toolholder

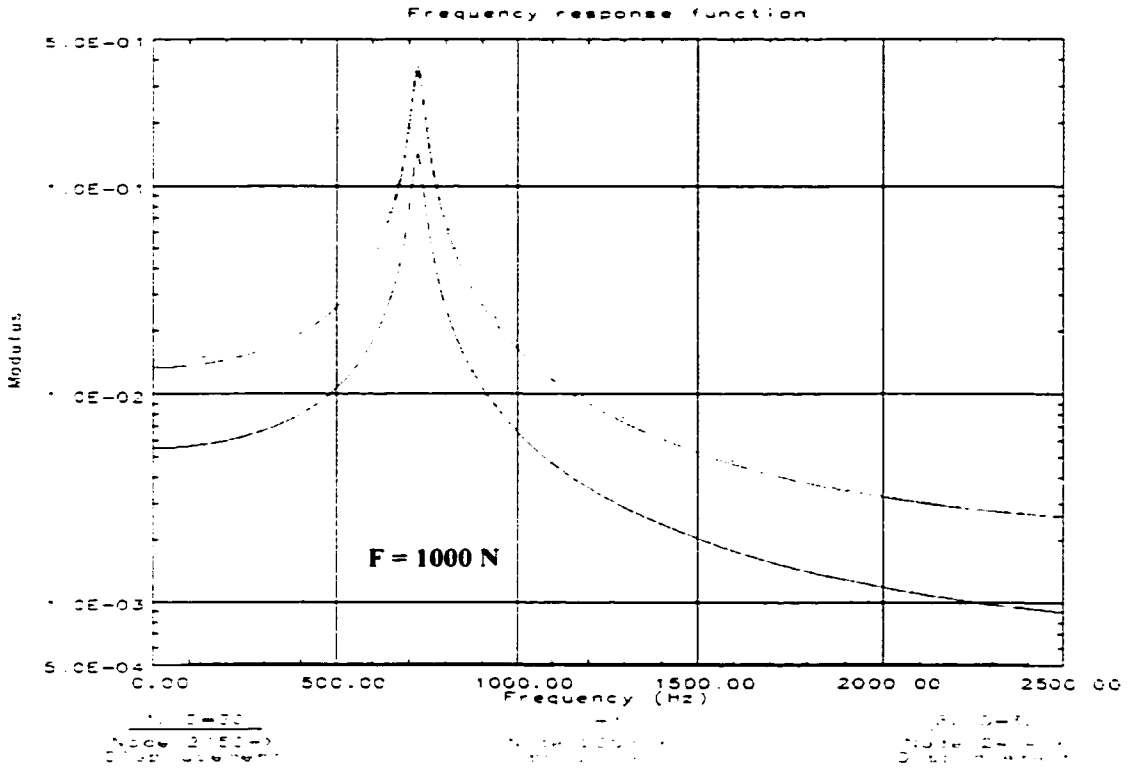

Figure 36 – Displacement Response for Medium Length Straight Shank Toolholder

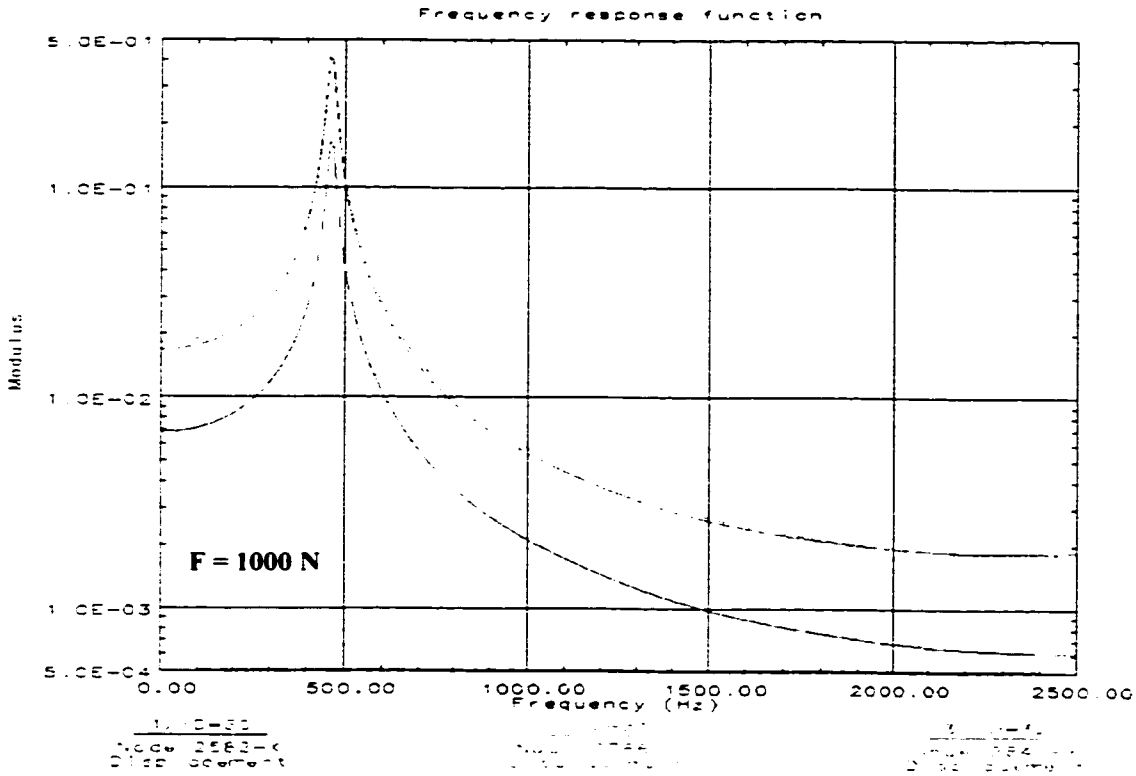

Figure 37 – Displacement Response for Long Length Straight Shank Toolholder

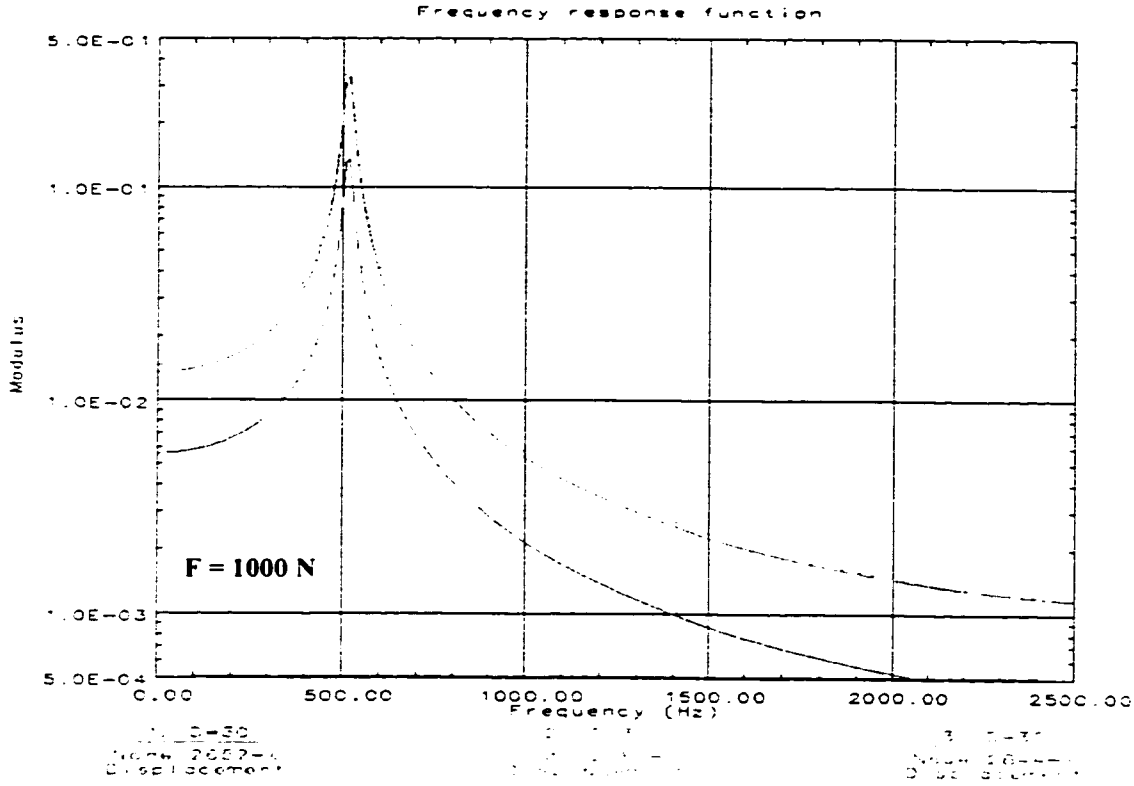

Figure 38 – Displacement Response for Large Diameter Straight Shank Toolholder

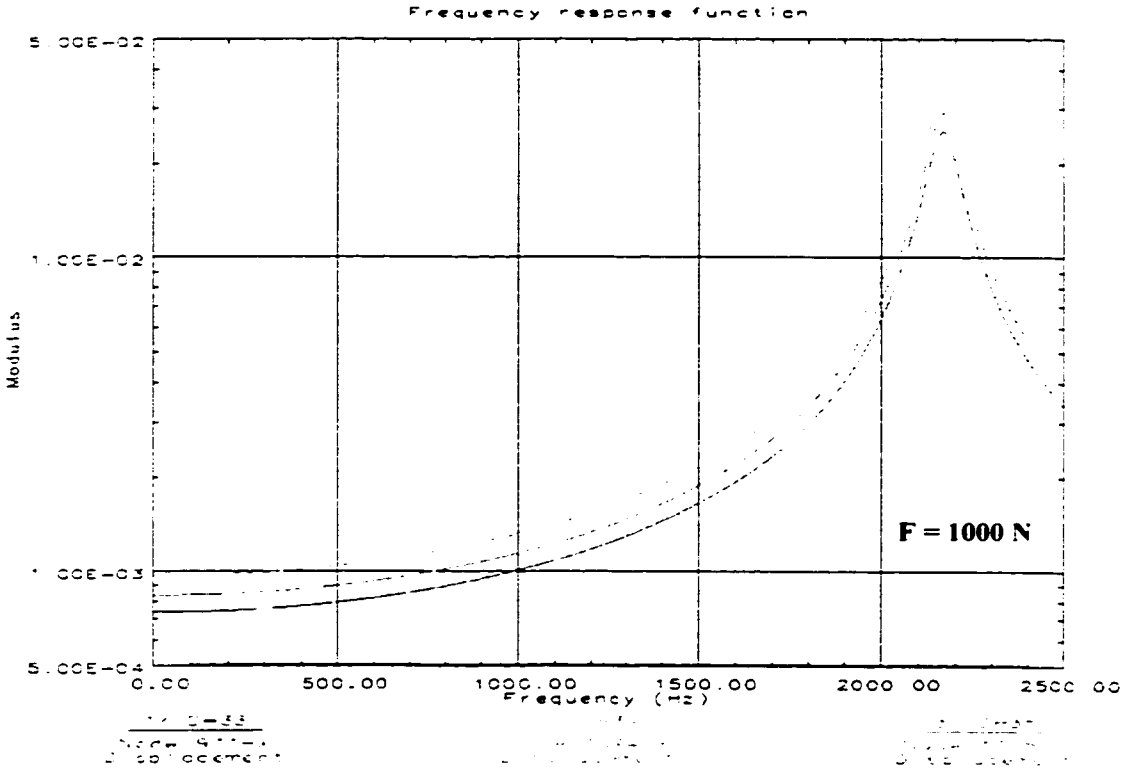

Figure 39 – Displacement Response for Short Length Tapered Shank Toolholder

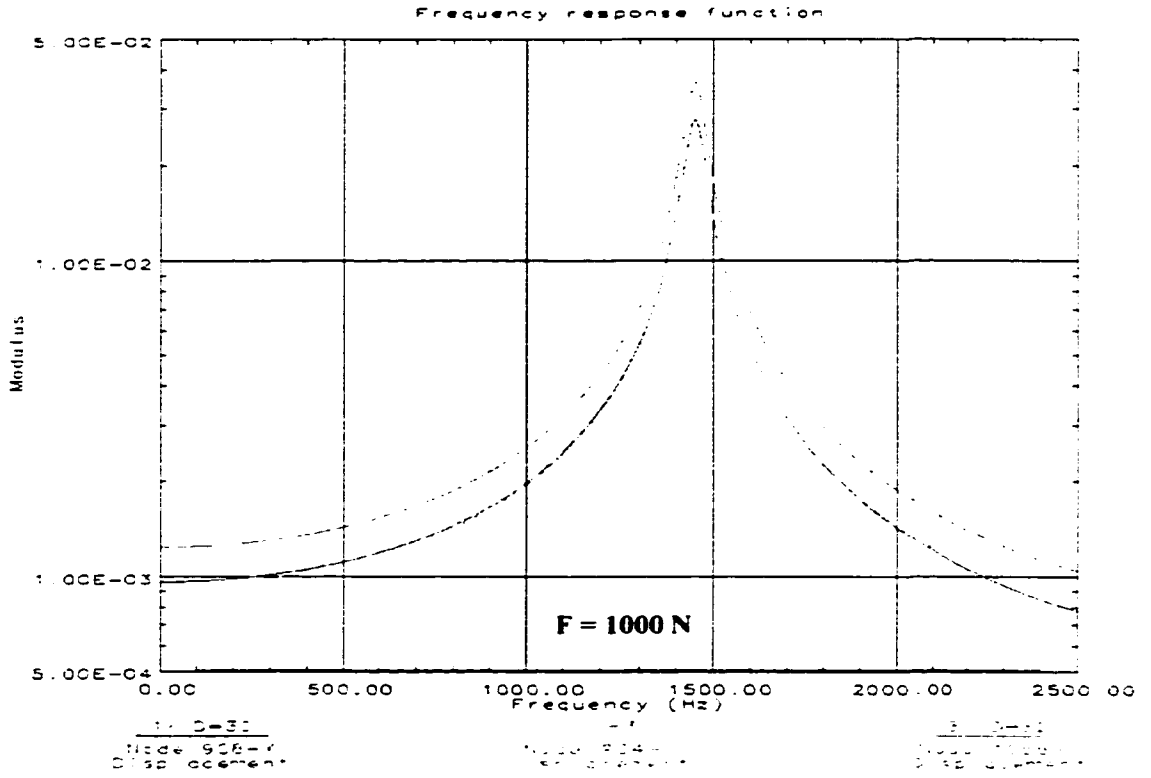

Figure 40 – Displacement Response for Long Length Tapered Shank Toolholder

before the slope begins to drastically increase. With the long toolholder, the frequency is only about 100 Hz before the slope changes. The implication of this is that the shorter toolholder can operate over a broader range of frequencies without its deflections changing significantly (less than .005 mm). The longer toolholder has a much narrower range. Once the operating frequency passes the 'flat' section and approaches resonance, a small change in frequency results in a large change in displacement.

When comparing the results between the medium length toolholder and the larger bodied toolholder of the same length (referred to as 'Wide' in the table), there is very little difference in the shank deflection at the lower frequency spectrum (below 200 Hz). As just discussed, stiffness plays the dominant role in the lower frequency range. Although the larger diameter toolholder has a much stiffer body, the stiffness in the shank has remained unchanged and is the same for all the straight shank toolholders. Referring to Figure 41, there is a clearance between the flange of the toolholder and the spindle. This will allow the toolholder to bend about its shank, which has a smaller moment of

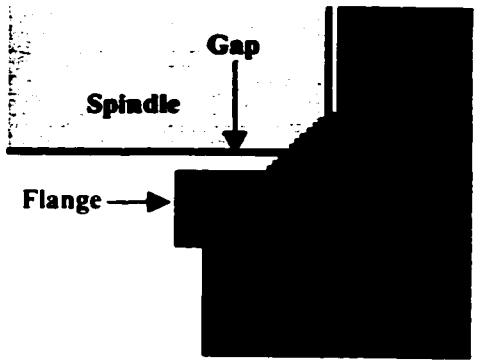

Figure 41 – Gap Between Flange and Spindle

inertia. The moment of inertia is an indicator of a beam's resistance to bending; the greater the value, the greater the resistance. For a circular cross-section, the moment of

inertia is proportional to the fourth power of the radius. As a result, even a small difference in diameter can significantly change this value. Since the toolholders are identical in length, the moment generated by the force is the same, resulting in similar deflections in the shank. The extra mass of the larger diameter toolholder does play a role by reducing the natural frequency. As the operating frequency increases, deflections will become much greater, much more quickly, than with smaller bodied toolholder.

The cutting force exerted on the tool is controlled by many factors including spindle speed, feed rate and depth of cut. The fact that deflections in the shank increase with increasing cutting force suggests an obvious solution; reduce the cutting load. With a low enough load, there is no need to worry about excessive deflections. However, this would not be a popular solution as the loss in productivity might significantly outweigh the benefit of reduced fretting damage.

There may be another force that can contribute to the deflection of the toolholder. If the toolholder is not perfectly balanced, an unbalance force will result causing significant deflections at higher speeds. In order to see to see how a potential unbalance would affect fretting, an eccentric mass of 10 g was applied to the middle of the short toolholder and spaced 20 mm from the centerline. With the toolholder weighing approximately 1200 g, the eccentric mass accounts for less than one percent of the total mass. Note that the unbalance was applied in addition to the 1000 N force. The frequency response function is shown in Figure 42. Since the unbalance force is related to the square of the speed, there is not much difference in deflections of the shank at the lower end of the spectrum. However, as the frequency increases there are significant differences. Therefore, with respect to fretting, an unbalance force is not a great

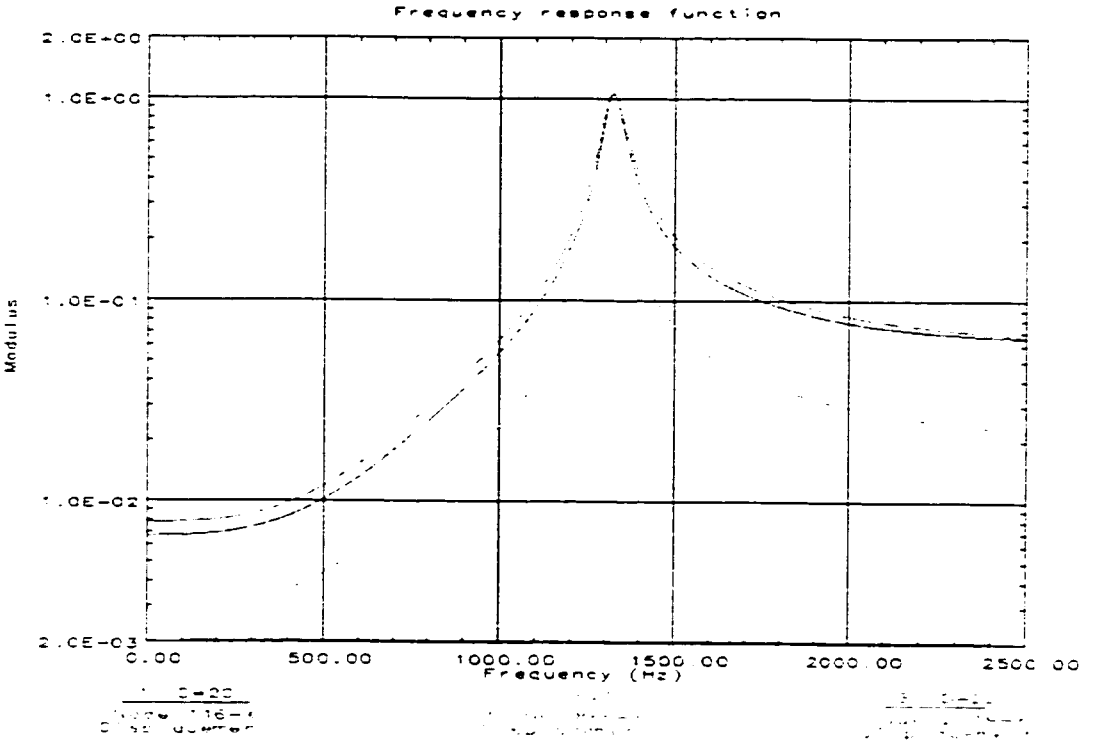

Figure 42 – Effect of Unbalance on Short Straight Shank Toolholder

concern unless spindle speeds are high. With respect to machining quality, though, an unbalanced toolholder should always be of concern.

D. Experimental Tests

Since the shank is hidden within the spindle, it would be very difficult to try to measure its dynamic displacement during actual machining. It would then be impossible to verify the accuracy of the model response results. Tests can be run, though, to show that the shank is actually bending. This involves the use of a blue ink that comes in a paste form (a brand name is Hi-Spot®). It is typically used by mold and die makers to check for high spots (or unevenness) between the surfaces of assembled parts. A thin coat of ink is applied to one of the surfaces and then the parts are assembled together. When disassembled, the ink pattern transferred to the other surface would indicate any unevenness between the surfaces.

For this test, the blue ink was applied to the spindle pocket. The toolholder was then inserted into the spindle and removed immediately. This was done to check the initial transfer of ink to the shank. If the layer of ink was thin enough, it should only transfer to those areas that come into direct contact with the spindle, namely the two bands at the upper and lower portion of the shank as seen in Figure 43. If the layer was too thick (thicker than the gap), the ink would transfer to the entire length of the shank. After the initial ink transfer was satisfactory, the toolholder was carefully re-inserted into the spindle to begin the cutting tests.

A tapered shank toolholder with a body length of 80 mm and a tool diameter of 3/4" was used to perform milling tests on a block of 1018 steel. The variables that were kept constant during the tests were the spindle speed (set to 1000 rpm) and the feed rate (set to 5 in/min). The only variable that changed was the depth of cut, which would determine the applied force. The test began by milling at a depth of 1/4" for several minutes. The toolholder was then removed from the spindle to check for any ink transfer. Any new ink would prove that fretting occurred. However, there was no sign of any ink transfer. The surfaces of the spindle and toolholder were then cleaned and a new layer of ink was applied to the spindle pocket. The procedure was repeated with a depth of cut of 1/2". At this depth there was substantial amounts of ink transfer (see Figure 44) indicating that contact did occur. According to the simulation results in Table 6, the small deflections of the tapered toolholder indicate that it is very stiff. It was, therefore, no surprise that a

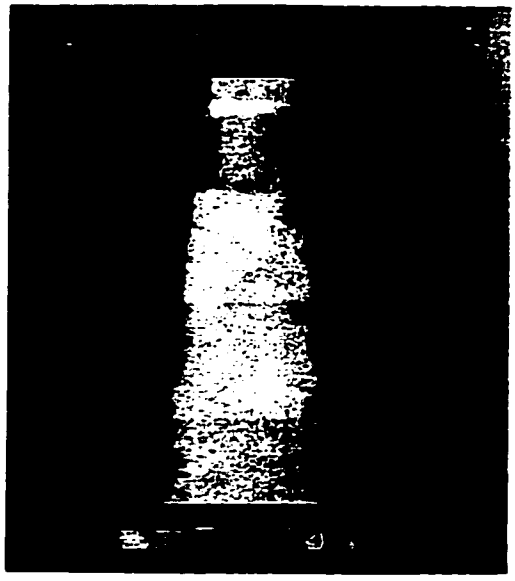

Figure 43 – Initial Ink Transfer

Figure 44 – Ink Transfer after Machining

large cutting force was required to cause the shank to deflect significantly.

An important consideration should be noted, however. By applying ink to the spindle, the thickness of the ink layer would effectively decrease the gap spacing. Although the test proved the shank deflected, the only conclusion that can be drawn is that it made contact with the ink and not necessarily the spindle.

VI. Conclusions

Based on the work presented in this thesis it was found that shank deflections could be controlled by altering the toolholder's design. Through the testing of two different toolholder types (straight and tapered shank), the following conclusions can be made relating design modifications to shank deflections at typical operating frequencies (below 200 Hz)

1) Shank deflections decrease as the length of a toolholder decreases. This is a result of stiffness being inversely proportional to length. Thus, shorter toolholders are stiffer than longer toolholders and would consequently deflect less under the same load.
2) Shank deflections were not significantly affected by changes to the body diameter. It was found that the toolholder bends about its shank. Since the shank diameter was constant within each type, increasing the body diameter, in an attempt to increase overall stiffness, had little effect.
3) Shank deflections were much less in the tapered shank designs than in the straight shank designs. At the point of bending, the shank diameter of the tapered design is much larger than the shank diameter in the straight design. As a result, tapered shank toolholders have a greater stiffness.

It is hoped that the results obtained through this work will be a useful guide in designing (or selecting) a toolholder that will minimize shank deflections, and thus minimize the chance of fretting.

References

[1] Archard, J. F., *Wear Theory and Mechanisms*, Wear Control Handbook, American Society of Mechanical Engineers, New York, 1980.

[2] Aronson, Robert B., *Machine Tool 101: Part 3, Spindles and Motors*, Manufacturing Engineering, March 1994.

[3] Aronson, Robert B., *Machine Tool 101: Part 4, Tools and Holders*, Manufacturing Engineering, April 1994.

[4] Brinkman, Brett A., Macioce, David J., *Understanding Modal Parameters and Mode Shape Scaling*, Sound and Vibration, June 1985.

[5] Bhansali, Kirit, J., *Wear Coefficients of Hard-Surfacing Materials*, Wear Control Handbook, American Society of Mechanical Engineers, New York, 1980.

[6] Brown, Dave, *Weaknesses of Impact Testing*, Proceedings of the 15th International Modal Analysis Conference, Society for Experimental Mechanics, Inc., Connecticut, 1997.

[7] Dossing, Ole, *Structural Testing, Part II: Modal Analysis and Simulation*, Bruel and Kjaer, 1988.

[8] Gaydos, P. A., Eiss, N. S., Furey, M. J., Mabie, H. H., *Fretting Wear of Polymeric Coatings, Wear Control Handbook*, American Society of Mechanical Engineers, New York, 1980.

[9] Godfrey, Douglas, *Diagnosis of Wear Mechanisms*, Wear Control Handbook, American Society of Mechanical Engineers, New York, 1980.

[10] Halvorsen, William G., Brown, David L., *Impulse Techniques for Structural Frequency Response Testing, Sound and Vibration*, November 1997.

[11] Inman, Daniel J., *Engineering Vibration*, Prentice Hall, New Jersey, 1994.

[12] Iwabuchi, Akira, *The Role of Oxide Particles in the Fretting Wear of Mild Steel, Wear of Materials*, American Society of Mechanical Engineers, New York, 1991.

[13] Kelly, S. G., *Fundamentals of Mechanical Vibrations*, McGraw Hill, New York, 1993.

[14] Ko, P. L., *A Brief Review of Tube Fretting-Wear in Heat Exchangers*, Atomic Energy of Canada Limited, 1984.

[15] McHargue, Patrick L., Richardson, Mark H., *Operating Deflection Shapes from Time Versus Frequency Domain Measurements*, Proceedings from the 11th International Modal Analysis Conference, Society for Experimental Mechanics, Inc., 1993.

[16] Myers, Michael J., *Toolholder Performance in the Balance*, Modern Machine Shop, January 1994.

[17] Potter, Ron, Richardson, Mark, *Mass, Stiffness, and Damping Matrices from Measured Modal Parameters*, ISA 74 International Instrumentation-Automation Conference and Exhibit, 1974.

[18] Schmidtberg, Rupert, Pal, Thomas, *Solving Vibration Problems Using Modal Analysis*, Sound and Vibration, March 1986.

[19] Sibley, L. B., *Roller Bearings*, Wear of Materials, American Society of Mechanical Engineers, New York, 1991.

[20] Singleton, Ken, *Tutorial on Experimental Modal Analysis*, Vibrations, June 1995.

[21] Thomson, William T., *Theory of Vibration with Applications, 3rd Ed.*, Prentice Hall, 1988.

[22] Van Karsen, Charles D., Little, Eric F., *The Strengths of Impact Testing*, Proceedings of the 15th International Modal Analysis Conference, Society for Experimental Mechanics, Inc., Connecticut, 1997.

[23] Vingsho, O., Odfalk, M., Shen, N. E., *Fretting Maps and Fretting Behaviour of Some FCC Metal Alloys*, Wear of Materials, American Society of Mechanical Engineers, New York, 1991.

Vita Auctoris

Name:	Joseph Jouraij
Place of Birth:	Leamington, Ontario, Canada
Year of Birth:	1972
Education:	University of Windsor Windsor, Ontario, Canada 1991-1995 B.A.Sc. Mechanical Engineering (Honours)